We are IntechOpen, the world's leading publisher of Open Access books Built by scientists, for scientists

4,800
Open access books available

122,000
International authors and editors

135M
Downloads

Our authors are among the

154
Countries delivered to

TOP 1%
most cited scientists

12.2%
Contributors from top 500 universities

CLARIVATE ANALYTICS BOOK CITATION INDEX INDEXED

WEB OF SCIENCE™

Selection of our books indexed in the Book Citation Index in Web of Science™ Core Collection (BKCI)

Interested in publishing with us?
Contact book.department@intechopen.com

Numbers displayed above are based on latest data collected.
For more information visit www.intechopen.com

Chapter 14

Alkaline and Alkaline-Earth Ceramic Oxides for CO_2 Capture, Separation and Subsequent Catalytic Chemical Conversion

Margarita J. Ramírez-Moreno,
Issis C. Romero-Ibarra, José Ortiz-Landeros and
Heriberto Pfeiffer

Additional information is available at the end of the chapter

http://dx.doi.org/10.5772/57444

1. Introduction

The amounts of anthropogenic carbon dioxide (CO_2) in the atmosphere have been raised dramatically, mainly due to the combustion of different carbonaceous materials used in energy production, transport and other important industries such as cement production, iron and steelmaking. To solve or at least mitigate this environmental problem, several alternatives have been proposed. A promising alternative for reducing the CO_2 emissions is the separation and/or capture and concentration of the gas and its subsequent chemical transformation. In that sense, a variety of materials have been tested containing alkaline and/or alkaline-earth oxide ceramics and have been found to be good options.

The aforementioned ceramics are able to selectively trap CO_2 under different conditions of temperature, pressure, humidity and gas mixture composition. The influence of those factors on the CO_2 capture (physically or chemically) seems to promote different sorption mechanisms, which depend on the material's chemical composition and the sorption conditions used. Actually, this capture performance suggests the feasibility of these kinds of solid for being used with different capture technologies and processes, such as: pressure swing adsorption (PSA), vacuum swing adsorption (VSP), temperature swing adsorption (TSA) and water gas shift reaction (WGSR). Therefore, the fundamental study regarding this matter can help to elucidate the whole phenomena in order to enhance the sorbents' properties.

2. CO_2 capture by different alkaline and alkaline-earth ceramics

Among the alkaline and/or alkaline-earth oxides, various lithium, sodium, potassium, calcium and magnesium ceramics have been proposed for CO_2 capture through adsorption and chemisorption processes [1-20]. These materials can be classified into two large groups: dense and porous ceramics. Dense ceramics mainly trap CO_2 chemically: the CO_2 is chemisorbed. Among these ceramics, CaO is the most studied one. It presents very interesting sorption capacities at high temperatures ($T \geq 600$ °C). In addition to this material, alkaline ceramic oxides have been considered as possible captors, mostly lithium and sodium based ceramics (Li_5AlO_4 and Na_2ZrO_3, for example). In these cases, one of the most interesting properties is related to the wide temperature range in which some of these ceramics trap CO_2 (between 150 and 800 °C), as well as their high CO_2 capture capacity.

In these ceramics, the CO_2 capture occurs chemically, through a chemisorption process. At a micrometric scale, a general reaction mechanism has been proposed, where the following steps have been established: Initially, CO_2 reacts at the surface of the particles, producing the respective alkaline or alkaline-earth carbonate and in some cases different secondary phases. Some examples are:

$$Li_5AlO_4 + 2\,CO_2 \longrightarrow 2Li_2CO_3 + LiAlO_2 \quad (1)$$

$$Na_2ZrO_3 + CO_2 \longrightarrow Na_2CO_3 + ZrO_2 \quad (2)$$

$$CaO + CO_2 \longrightarrow CaCO_3 \quad (3)$$

The above reactions show that surface products can be composed of carbonates, but as well they can contain metal oxides or other alkaline/alkaline-earth ceramics. The presence of these secondary phases can modify (improve or reduce) the diffusion processes described below [1].

Once the external carbonate shell is formed, different diffusion mechanisms have to be activated in order to continue the CO_2 chemisorption, through the particle bulk. Some of the diffusion processes correspond to the CO_2 diffusion through the mesoporous external carbonate shell, and some others such as the intercrystalline and grain boundary diffusion processes [1, 18, 21].

Figure 1 shows the theoretical CO_2 chemisorption capacities (mmol of CO_2 per gram of ceramic) for the most studied alkaline and alkaline-earth ceramics. As it can be seen, metal oxides (Li_2O, MgO and CaO) are among the materials with the best CO_2 capture capacities. Nevertheless, Li_2O and MgO have not been really considered as possible options due to reactivity and kinetics factors, respectively. On the contrary, CaO is one of the most promising alkaline-earth based materials, with possible real industrial applications. Other interesting materials are ceramics with lithium or sodium phases, which present better thermal stabilities and volume variations

http://dx.doi.org/10.5772/57444

than CaO. In addition, the sodium phases may present another advantage if the CO_2 capture is produced in the presence of steam. Under these conditions the sodium phases may produce sodium bicarbonate ($NaHCO_3$) as the carbonated phase, which is twice the amount of CO_2 could be trapped in comparison to the Na_2CO_3 product.

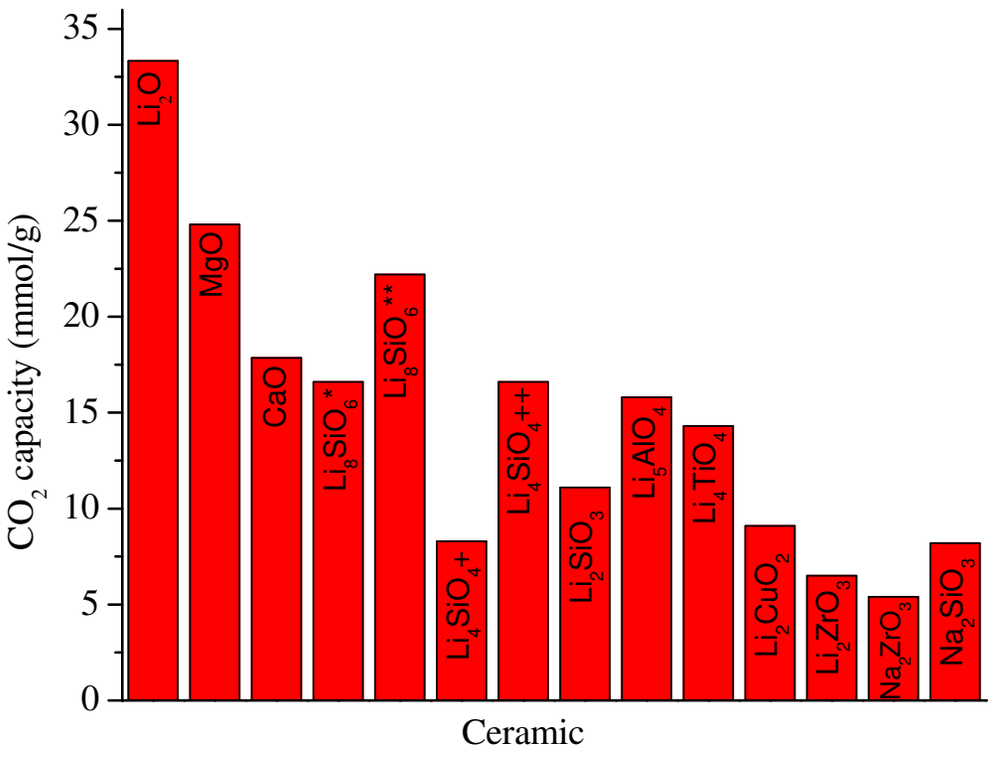

Figure 1. Theoretical CO_2 capture capacities for different alkaline and alkaline-earth ceramics. In the Li_8SiO_6 (labeled as *) and Li_4SiO_4 (labeled as +), the maximum capacity can depend on the CO_2 moles captured in each different phase formed ($Li_8SiO_6 + CO_2 \rightarrow Li_4SiO_4 + CO_2 \rightarrow Li_2SiO_3 + Li_2CO_3$).

Other ceramics containing alkaline-earth metals are the layered double hydroxides (LDH) or hydrotalcite-like compounds (HTLc). LDHs, also called anionic clays due to their layered structure and structural resemblance to a kind of naturally-occurring clay mineral. These materials are a family of anionic clays that have received much attention in the past decades because of their numerous applications in many different fields, such as antacids, PVC additives, flame retardants and more recently for drug delivery systems and as solid sorbents of gaseous pollutants [22-24]. The LDH structure is based on positively charged brucite like $[Mg(OH)_2]$ layers that consist of divalent cations surrounded octahedrally by hydroxide ions. These octahedral units form infinite layers by edge sharing [25]. Due to the fact that certain fraction of the divalent cations can be substituted by trivalent cations at the centers of octahedral sites, an excess of positive charge is promoted. The excess of positive charge in the main layers of LDHs is compensated by the intercalation of anions in the hydrated interlayer space, to form the three-dimensional structure. These materials have relatively weak bonds between the interlayer and the sheet, so they exhibit excellent ability to capture organic or inorganic anions. The materials are easy to synthesize by several methods such as co-precipitation,

rehydration-reconstruction, ion exchange, hydrothermal, urea hydrolysis and sol gel, although not always as a pure phase [26].

The LDH materials are represented by the general formula: $\left[M^{II}_{1-x}M^{III}_{x}(OH)_2\right]^{x+}\left[A^{m-}\right]_{x/m} \bullet nH_2O$ where M^{II} and M^{III} are divalent (Mg^{2+}, Ni^{2+}, Zn^{2+}, Cu^{2+}, etc.) and trivalent cations (Al^{3+}, Fe^{3+}, Cr^{3+}, etc.), respectively, and A^{m-} is a charge compensating anion such as CO_3^{2-}, SO_4^{2-}, NO_3^-, Cl^-, OH^-, where x is equal to the molar ratio of $[M^{III}/(M^{II} + M^{III})]$. Its value is commonly between 0.2 and 0.33, i.e., the M^{II}/M^{III} molar ratio is in the range of 4 - 2 [25], but this is not a limitation ratio and it depends on the M^{II} and M^{III} composition [27-29].

Among various CO_2 mesoporous adsorbents, LDH-base materials have been identified as suitable materials for CO_2 sorption at moderate temperatures ($T \leq 400$ °C) [30-46] due to their properties such as large surface area, high anion exchange capacity (2-3 meq/g) and good thermal stability [37-40]. The LDH materials themselves do not possess any basic sites. For that reason, it is preferred to use their derived mixed oxides, formed by the thermal decomposition of LDH, which do exhibit interesting basic properties. Thermal decomposition of the material occurs in three stages, first at temperatures lower than 200 °C, at which the dehydration of superficial and interlayer water molecules takes place on the material. Then the second decomposition stage takes place in the range of 300-400 °C, at which the structure collapses due to a partial dehydroxylation process, typically associated with both the decomposition of Al-OH and the Mg-OH hydroxides. During dehydroxylation, changes occur in the structure. A portion of the trivalent cations of the brucite like layers migrates to the interlaminar region, allowing the preservation of the laminar characteristics of the material [41]. Finally, the total decomposition of the material occurs at temperatures higher than 400 °C, when the decarbonation process is completed [42].

Once the temperature reaches about 400 °C, LDH forms a three-dimensional network of compact oxygen with a disordered distribution of cations in the interstices, where the cations M^{+3} are tetrahedrally coordinated (interlayer region) and M^{+2} are octahedrally coordinated. The compressive-expansion stresses associated with the formation of the amorphous three-dimensional networks and their connection to the octahedral layer increases the surface area and pore volume, which can help improve the storage capacity properties, for example for gas sorption related applications, besides decreasing the ability of the Mg^{+2} cation to favor physisorption instead of chemisorption [30, 42]. For instance, the thermal evolution of the Mg/Al-CO_3 LDH structure is considered to be crucial in determining the CO_2 adsorption capacity, so there are several studies about this issue [42-44].

Reddy et al. [43] studied the effect of the calcination temperature on the adsorptive capacity of the Mg/Al-CO_3 LDH. They found out that the best properties were obtained at calcination temperature of 400 °C, which they attributed to the obtaining of a combination of surface area and the availability of the active basic sites. Actually, at this temperature the material is still amorphous, which allows having a relatively high surface area. Therefore, there is a high number of exposed basic sites, allowing the reversible CO_2 adsorption according to the following reaction:

http://dx.doi.org/10.5772/57444

$$Mg\text{-}O + CO_2 \rightarrow Mg\text{-}O \cdots CO_2\ (ad) \quad (4)$$

However, if the LDH is calcined under 500 °C, the material is able to transform back to the original LDH structure when it is exposed to a carbonate solution or another anionic containing solution. Finally, if the sample is heated to temperatures above 500 °C, the structural changes become irreversible because of the spinel phase formation [37].

As mentioned, the mixed oxides derived from the LDH calcination possess some interesting characteristics such as high specific surface area, excess of positive charge that needs to be compensated, basic sites and thermal stability at elevated temperatures (200 – 400 °C). Besides these aspects, it is important to consider the advantage of acid-base interactions on the CO_2 sorption applications, where acidic CO_2 molecules interact with the basic sites on the derived oxide. These characteristics make the LDH-materials acceptable CO_2 captors [43, 45]. However, the CO_2 adsorption capacity of this material is low compared with other ceramic sorbents; reaching mean values smaller than 0.1 mmol/g [46]. Nevertheless, many studies suggest that the adsorption capacity of LDH materials can be improved by modifying a factor set such as: composition, improvement of the material's basicity and contaminant gas stream composition [30-32, 36, 41-45, 47-59].

As previously mentioned, Reddy et al. [43] studied the influence of the calcination temperature of LDHs on their CO_2 capture properties. The Mg_3/Al_1-CO_3 material was calcined at different temperatures ranging from 200 to 600 °C. The results showed that when the calcination temperatures are under 400 °C, LDH is considered to be dehydrated and materials still keep the layered structure intact, wherein the CO_3^{2-} ions are occupying the basic sites. The obtained samples calcined at 400 °C have the maximum BET surface area of 167 m^2/g compared with samples calcined at lower temperatures. Moreover, during the calcination of the LDH at higher temperatures (T > 500 °C), most of the CO_3^{2-} decompose to release some basic sites for CO_2 adsorption. However, the final amount of basic sites decreases with the subsequent crystallization of the MgO and spinel ($MgAl_2O_4$). Hence, LDH materials obtained at 400 °C have the highest surface area and the maximum quantities of active basic sites exposed. Because of these characteristics, they achieved a total sorption capacity of 0.5 mmol/g [43]. The same researchers observed that 88% of the captured gas can be desorbed and during the material regeneration 98% of the original weight is gained. This is another important property of LDH materials in high temperature CO_2 separation applications as described later..

As mentioned, the thermal evolution of the layered structure has a great influence on the CO_2 capture. The loss of superficial interlayer water occurs at 200 °C. Then at temperatures between 300 and 400 °C the layer decomposition begins, resulting in an amorphous 3D network with the highest surface area [30], so the adsorption temperature improves the CO_2 capture in the order of 400 > 300 > 20 >200 °C [41-42, 47, 52]

Several researchers have investigated a set of different factors to improve the CO_2 sorption capacity. Yong et al. [47, 48] studied the factors which influence the CO_2 capture in LDH materials, such as aluminum content, water content and heat treatment temperature. Regarding the M/Al-CO_3 LDHs (M = Mg, Ni, Co, Cu or Zn), the best CO_2 sorption capacity was

obtained for the Mg/Al materials degassed at 400 °C and with adsorption conditions of 25 °C. In general, the sorption capacity follows the trend Ni > Mg > Co > Cu = Zn. However, when the degassed temperature is increased, the trend is modified to Mg (400 °C) > Co (300°C) > Ni (350°C) > Cu (300°C) >Zn (200°C). These results show that Mg/Al-CO_3 is the best composition at the degassing temperature of 400 °C [47]. At this temperature, the material consists of an amorphous phase with optimal properties for use as CO_2 captor [42]. Also, the influence of Al^{+3} has been studied as a trivalent cation at 25 and 300 °C adsorption temperatures, by Yong [41] and Yamamoto [49] respectively. Both samples were degassed at 300 °C and the results showed that the CO_2 capture is influenced by the adsorption temperature. At a temperature of 25 °C, the maximum adsorption was 0.41 mmol/g with an Mg/Al ratio equal to 1.5 (x = 0.375) [41] and at 300 °C the amount of CO_2 adsorbed was 1.5 mmol/g for a cation ratio of 1.66 (x = 0.4) [49]. The differences between the two capacities can be attributed to the Al content differences. The Al incorporation in the structure has two functions: 1) to increase the charge density on the brucite-like sheet; and 2) to reduce the interlaminar distance and the number of sites with high resistance to CO_2 adsorption [48].

On the other hand, Qian et al. [50] studied the effect of the charge compensation anions (A^- = CO_3^{-2}, NO_3^{-1}, Cl^-, SO_4^{-2} and HCO_3^{-1}) on the structural properties and CO_2 adsorption capacity of Mg/Al-A^- (molar ratio equal to 3). Despite all of the prepared LDH materials showed the typical XRD patterns of LDH materials, slight structural and microstructural differences were observed. In fact, the interlayer distance changed by varying the interlayer anions due to their difference in sizes and carried charges. These differences affect the morphology and the BET surface area of both fresh and heat-treated LDH materials. Additionally, thermal treatments were performed in order to optimize the adsorption capacity of these materials. The optimal temperature treatment was established for each Mg/Al-A^- based on the surface area of each calcined LDH. Then the CO_2 adsorption capacities of calcined LDH were tested at 200 °C. Mg_3/Al_1–CO_3 showed the highest CO_2 adsorption capacity (0.53 mmol/g). This value was much higher than those obtained for calcined Mg_3/Al_1-NO_3 > Mg_3/Al_1-HCO_3, Mg_3Al_1-Cl, and Mg_3/Al_1-SO_4 (≈ 0.1 mmol/g). The results indicated that BET surface area of calcined LDHs seems be the main parameter that determines the CO_2 adsorption capacity because the Mg-O active basic site [43, 45].

It has been demonstrated that the quasi-amorphous phase obtained by the thermal treatment of LDH at the lowest possible temperature has the highest CO_2 capture capacity. This finding is in line with the fact that high calcination temperature can decrease the number of active Mg–O sites due to the formation of crystal MgO [51].

Yong [41] and Yamamoto [49] investigated the influence of the several types of anions. The results suggested that the amounts CO_2 capture decrease as a function of the anion size, which promotes a larger interlayer spacing and the higher charge: $Fe(CN)_6^{4-}$(1.5 mmol/g) > CO_3^{2-} (0.5 mmol/g) > NO_3^- (0.4 mmol/g) > OH^- (0.4-0.25 mmol/g). The reason is that $Fe(CN)_6^{4-}$ and CO_3^{2-}, because they have more void space in the interlayer due size, and are able to accommodate higher CO_2 quantities. Calcined layered double hydroxide derivatives have shown great potential for high temperature CO_2 separation from flue gases. However, the presence of SOx and H_2O from flue gases can strongly affect CO_2 adsorption capacity and regeneration of

http://dx.doi.org/10.5772/57444

hydrotalcite-like compounds. Flue gases emitted from power stations contain considerable amounts of water in the form of steam. The percentage of water found in the flue gas emitted from different sources varies between 7 and 22%, with the emissions from brown coal combustion having the highest water content [45]. For many other gas adsorption sorbents, steam generally has a negative effect on the adsorption performance because of competition for basic sites between CO_2 and H_2O. However, the presence of water or steam seems to be favorable for the adsorption capacity onto LDH [31,43,53,54]. This fact is the result of the increasing potential energy that is able to further activate basic sites, possibly by maintaining the hydroxyl concentration of the surface material and/or preventing site poisoning through carbonate or coke deposition [31]. An example of the above was reported by Yong et al. [47], who found that water or steam can increase the adsorption capacity of CO_2 by about 25%, from 0.4 mmol/g to 0.5 mmol/g.

Ding et al. [31] studied CO_2 adsorption at higher temperatures (480 °C) under conditions for steam reforming of methane. They found an adsorption capacity of 0.58 mmol/g, which was independent of water vapor content in the feed. In turn, Reddy et al. [45] investigated calcined LDHs' sorption performance influenced by CO_2 wet-gas streams. LDH samples were calcined at 400 °C [43] before measuring CO_2 sorption at 200 °C. The gas streams used were CO_2, CO_2 + H_2O, flue gas (14% CO_2, 4% O_2 and 82 % N_2) +12% H_2O.

For a pure CO_2 dry sorption, the maximum weight gain was 2.72% (~0.61 mmol/g) after 60 min, whereas the wet adsorption increased the weight of the calcined LDHs to 4.81%, showing an additional 2.09%, where He and He + H_2O were used to remove the H_2O water capture. The results showed that the helium has virtually no significant sorption affinity for the material, whereas the water-sorption profile of it clearly indicates a water weight gain of 1.67%, i.e., the gain was 0.1mmol/g due to steam presence, showing that water has a positive effect, shifting the CO_2 sorption by 0.42% as compared to dry CO_2 sorption. Also, these results revealed that in all cases about 70% sorption occurs during the first 5 min and reaches equilibrium after around 30 min.

To determine the influence of CO_2, Reddy et al. [43] tested a sample in both, wet and dry CO_2 stream conditions. The experiments showed that the same quantity of CO_2 can be trapped for the solid sorbent after two hours. The presence of water in the stream only affects the kinetics of the process. This result is in agreement with that reported by Ding et al. [31]. On the other hand, the results of the material tested suggest that the fact the CO_2 capture from flue gas was higher than in a pure stream of CO_2 might have been because the polluted gas was diluted in the stream. The presence of the water does not enhance de CO_2 capture; the maximum CO_2 adsorbed was 0.9 mmol/g. The differences between Reddy et al. results and the previously mentioned studies can be caused by the use of uncalcined LDHs, which already contain an -OH network.

To apply these materials in industrial processes, it is important to know the times during which each sorbent material can be used. Tests of the cyclability in LDH materials disclose that as function of the temperature the CO_2 capture time can vary. This can be attributed to CO_2 chemisorbed during each cycle [54] and/or to the formation of spinel-based aluminas, such as γ-Al_2O_3 (at temperatures higher than 400 °C). Hibino et al. [52] found that the carbonate

content, acting as charge-compensating anion, continuously decreases in subsequent calcination – rehydration cycles. Reddy et al. tested LDH materials during six CO_2 adsorption (200 °C)-desorption (300 °C) cycles. The average amount gained was 0.58 mmol/g, whereas 75% of this value is desorbed, reaching desorption equilibrium after the third cycle. This can be attributed to the stabilization of the material phase and basic sites during the temperature swing.

Hufton et al. [54] studied a LDH material during several cycles in dry and wet CO_2 flows. As previously discussed, the presence of steam in the flow gas improves the CO_2 adsorption. However, after 10 adsorption cycles, the capture decreased 45%. The same behavior was observed in the dry gas flow. However, the final capture was similar to the wet gas stream, in agreement with Reddy et al. [43].

Recent studies have demonstrated that K-impregnated LDH or K-impregnated mixed oxides have a better CO_2 capture capacity due to the addition of K alkaline-earth element that improves the chemical affinity between the acidic CO_2 and alkaline surface of the sorbent material [32, 36, 55-56]. Additionally, it has been proposed that K-impregnation reduces the CO_2 diffusion resistance in the material. [57]. Hufton et al. [58] showed that the K-impregnation increases the CO_2 capture, but there is an optimal quantity of K to reach the maximum capture. Qiang et al. [50] tested an Mg_3/Al_1-CO_3 (pH = 10) impregnated with 20 wt.% K_2CO_3. The CO_2 adsorption capacity was increased between 0.81 and 0.85 mmol/g in the temperature range of 300 - 350 °C. This adsorption capacity is adequate for application in water gas shift reactions (WGS).

Lee et al. [59] tested the behavior of three commercial LDHs impregnated with K (K_2CO_3/LDH ratio between 0 and 1). Three Mg/Al-CO_3 LDH with different contents of magnesium were used. Results indicated that the sorption capacity of the LDH is improved by about 10 times with the optimal K_2CO_3 additions. Additionally, it was observed that impregnation is not the only factor that influences the adsorption but the composition too. The best value was obtained when the content of divalent cation was reduced and therefore, the material had a composition with the maximum trivalent cation content. The CO_2 adsorption capacity improved from 0.1mmol/g to 0.95mmol/g with K_2CO_3/LDH weight ratio equal to 0.35 at 400 °C. After determining the optimal alkaline source/LDH ratio, a set of samples was evaluated as a function of the temperature and the results showed a maximum of 1.35 mmol/g, at 50 °C. In the impregnated materials, CO_2 chemisorption can occur and the sorbed CO_2 can be further stored as metal carbonate forms.

Other alkaline elements can be used to improve the sorption capacity of materials. Martunus et al. [46] studied the impregnation of LDH with Na and K. The LDH samples were thermally treated at 450 °C for 5 min then calcined samples were re-crystallized in K_2CO_3 and Na_2CO_3 (1 M) solutions. The re-crystallized materials were tested as CO_2 captors and the capture was maximum with LDH-Na (0.688 mmol/g) > LDH- K (0.575 mmol/g) at 350 °C after five cycles. Finally, the re-crystallized material with the highest capture was calcined at 650 °C for 4 h and re-crystallized with a solution containing the appropriate quantities of K and Na to achieve alkaline metal loading up to 20%. When the sample was Impregnated with additional K and Na at 18.4% and 1.6%, respectively, the adsorption capacity rose

http://dx.doi.org/10.5772/57444

from 0.688 to 1.21 mmol/g. This capacity increase was achievable despite the relatively low BET surface area, equal to 124 m^2/g.

Other alkaline elements such as cesium have been studied as reinforcement. Oliveira et al. [55] tested commercial Mg_1/Al_1-CO_3 and Mg_6Al_1-CO_3 impregnated with K and Cs carbonates. The materials were evaluated in the presence of steam (26% v/v water content) gas at different temperatures (306, 403 and 510 °C) at 0.4 bar of CO_2 partial pressure (total pressure 2 bar). The LDH with the highest sorption capacity was Mg_1/Al_1-CO_3–K with 0.76 mmol/g at 403 °C. Among the Cs impregnated samples, the Mg_6Al_1-CO_3-Cs presented the highest capacity with 0.41 mmol/g, while the commercial LDH samples presented CO_2 sorption capacities around 0.1 mmol/g.

The results suggest the existence of a sorption mechanism combining physical adsorption and chemical reaction. First the maximum physical adsorption is reached, then the chemisorption begins, but there is an optimal temperature. If the temperature is too low, the chemisorption does not happen, but with higher temperatures the loss of porosity impedes the contact of CO_2 molecules with active basic sites promoted by the alkaline element addition.

These results suggest there is an optimum amount of K_2CO_3 to impregnate the LDH that achieves a balance between the increase in the basicity of the sorbent material and its reduction of surface area, associated with CO_2 capture capacity. The influence of potassium is currently not clear and the relevant research is still ongoing. Finally, CO_2 adsorption capacity on the synthesized 20 wt.%$K_2CO_3/Mg_3/Al_1$–CO_3 (pH = 10) probably could be further increased in the presence of steam.

3. Ceramic oxide membranes as an alternative for CO_2 separation

Membrane-based processes, related to gas separation and purification, have achieved an important level of development for a variety of industrial applications [60]. Therefore, the use of separation membranes is one of the promising technologies for reducing the emissions of greenhouse gases such as CO_2. The term membrane is defined as a permselective barrier between two phases, the feed or upstream and permeate or downstream side [61]. This permselective barrier has the property to control the rate of transport of different species from the upstream to the downstream side, causing the concentration or purification of one of the species present in the feed gas mixture.

Membrane-based processes offer the advantage of large scale application to separate CO_2 from a gas mixture. Figure 2 schematizes the process where concentrated CO_2 is selectively separated from flue gas that is mainly composed of nitrogen and carbon dioxide along with other gases such as water vapor, SO_x, NO_x and methane. Subsequent to the membrane process, concentrated CO_2 obtained at the permeate side can be disposed or used as raw material for the synthesis of several chemicals such as fuel and value-added products [62].

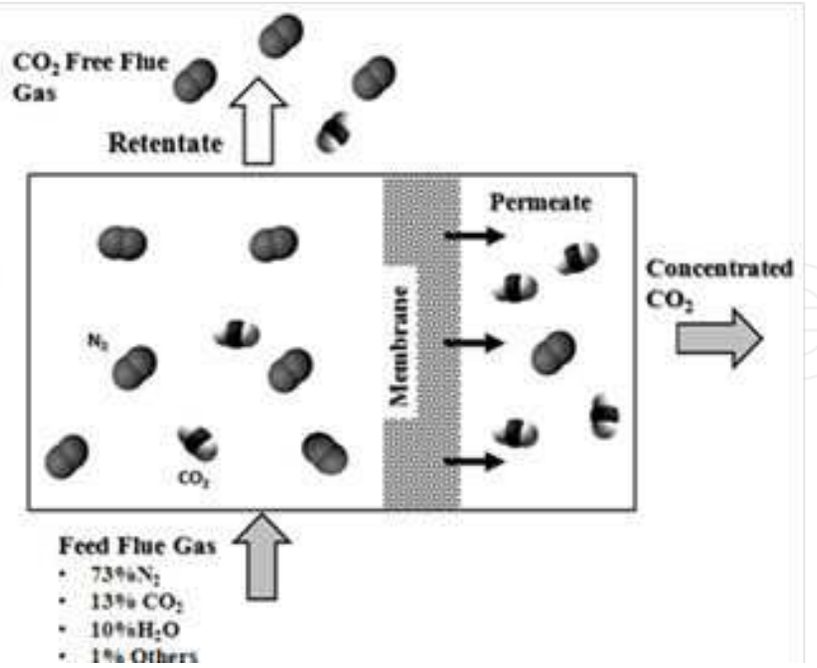

Figure 2. Membrane-based processes for the carbon dioxide separation from flue gases. The concentrated CO_2 is obtained in the permeate side.

Of course, the rate of transport or permeation properties of a particular gas through a given membrane depend on the nature of the permeant gas, as well as the physical and chemical properties of the membrane.

Inorganic membranes are more thermally and chemically stable and have better mechanical properties than organic polymer membranes; ceramic membranes offer both the advantage of large scale application and potential for pre- and post-combustion CO_2 separation applications, where membranes systems would be operating at elevated temperatures of 300-1000 °C [63].

Inorganic ceramic membranes can be classified as porous and nonporous or dense. These differ from each other not only in their structures but also in the mechanism of permeation. In porous membranes, the transport of species is explained with the pore-flow model, in which permeants are transported by pressure-driven convective flow through the pore network. Separation occurs because one of the permeants is excluded (molecular filtration or sieving) from the pores in the membrane and remains in the retentate while the other permeants move towards the downstream side. On the other hand, in nonporous membranes, separation occurs by solution-diffusion, in which permeants dissolve in the membrane material and then diffuse through the bulk membrane by a concentration gradient [60].

3.1. Porous membranes based on alkaline and alkaline-earth ceramic oxides for CO_2 separation

Among the porous systems for CO_2 separation, both microporous (carbon, silica and zeolite membranes) and modified mesoporous membranes have been reported [63-64].

http://dx.doi.org/10.5772/57444

Zeolites are hydrous crystalline aluminosilicates that exhibit an intracrystalline microporous structure as a result of the particular three-dimensional arrangement of their TO_4 tetrahedral units (T=Si or Al) [65]. Zeolite membranes are commonly prepared as thin films grown on porous alumina supports via hydrothermal synthesis and dry gel conversion methods [66]. Zeolite membranes of different structures have been developed to separate CO_2 from other gases via molecular sieving [67-69]. For example, membranes prepared with the 12-member ring faujasite (FAU)-type zeolite show high separation factors of 20-100 for binary gas mixtures of CO_2/N_2 [69]. In the same sense, T zeolite membranes exhibited very high selectivity, of about 400, for CO_2/CH_4 and 104 for CO_2/N_2. The high selectivity of CO_2/CH_4 exhibited by T zeolites is due to the small pore size of about 0.41 nm, which is similar in size to the CH_4 molecule but larger than CO_2 [69]. Table 1 shows the kinetic diameter of various molecules that are present in CO_2 containing gas mixtures such as flue and natural gas [70].

Molecule	Kinetic diameter (Å)
H_2O	2.65
H_2	2.69
CO_2	3.3
O_2	3.46
N_2	3.64
CH_4	3.80

Table 1. Kinetic diameter of various molecules based on the Lennard Jhones relationship.

Deca-dodecasil 3R (DDR) (0.36 nm x 0.44 nm), and pseudo-zeolite materials like silicoaluminophosphate (SAPO)-34 (0.38 nm) also show high CO_2/CH_4 selectivities due to narrow molecular sieving, which controls molecular transport into this material [69, 71-73]. For example, Tomita et al. [74] obtained a CO_2/CH_4 separation factor of 220 and CO_2 permeance values of 7×10^{-8} mol m^{-2} s^{-1} Pa^{-1} at 28 °C on a DDR membrane [75].

As discussed, one of the most important factors controlling permeation through microporous membranes is the restriction imposed by the molecular size of the permeant. However, the transport mechanism in microporous systems is more complex than just size exclusion and the permeation and selectivity properties are also affected by competitive adsorption among perment species that produce differences in mobility [76].

Thus, the diffusion mechanism for gas permeation through microporous membranes can be characterized by two modes: one controlled by adsorption and a second one where diffusion dominates [63]. In the case of adsorption-controlled mode with permeating gases having strong affinity with the membrane, a gas permeation flux equation is obtained by assuming steady-state single gas permeation, a constant diffusivity and a single gas adsorption described by a Langmuir-type adsorption isotherm, as in Eq. (5).

$$J = \phi q_s \frac{D_c}{L}\left(\frac{1 + bP_f}{1 + bP_p}\right) \text{ or } J = \phi q_s \frac{D_c}{L}\left(\frac{1 - \theta_p}{1 + \theta_f}\right) \quad (5)$$

where J is the permeation flux, ϕ is a geometric correction factor that involves both membrane porosity and tortuosity, D_c is the corrected diffusivity of the permeating species, L is the membrane thickness, P_f and P_p represent the feed and permeate pressure respectively and θ_f and θ_p represent the relative occupancies.

Furthermore, if the adsorption isotherm of the permeating gas is linear (1 >> bP), then flux permeation is described by Eq. (6).

$$F = \phi q_s \frac{D_c}{L}\left(\frac{D_c}{L}\right)K \quad (6)$$

where F is the permeance and $K = q_s b$ is the adsorption equilibrium constant. Therefore, from Eq. (5) it can be concluded that permeance is determined by both diffusivity (Dc) and adsorption (K). Based on the above, an interesting option to enhance membrane properties is to intercalate zeolite membranes with alkaline and alkaline-earth cations. Zeolite intercalation can enhance the separation between CO_2 and other molecules such as N_2 by promoting preferential CO_2 adsorption [63, 77]. It is well known that zeolites show affinity for polar molecules, like CO_2, due to the strong interaction of their quadrupole moment with the electric field of the zeolite framework. In this sense, the adsorption properties of zeolites can be enhanced by the inclusion of exchangeable cations within the cavities of zeolites where the adsorbent-adsorbate interactions are influenced by the basicity and electric field of the adsorbent cavities [78-80]. Lara-Medina et al. [77] carried out separation studies of CO_2 and N_2 with a silicalite-1 zeolite membrane prepared via hydrothermal synthesis and subsequently modified by using lithium solutions in order to promote preferential CO_2 adsorption and diffusion. CO_2/N_2 separation factor increases from 1.46 up to 6 at 25 psi and 400 ◦C after lithium modification. An et al. [79] studied a series of membranes prepared starting from natural Clinoptilolite zeolite rocks. Disk membranes were obtained by cutting and polishing of the original minerals, which were subsequently chemically treated with aqueous solutions containing Li, Na, Sr or Ba ions. Ionic exchanged membranes showed better permeation properties due to the presence of the extra framework cations.

Although zeolite membranes offer certain advantages in comparison with polymer membranes, such as chemical stability, the main issues are related to the selectivity decrease as a function of the permeation temperature. This is explained in terms of the contribution of the adsorption to the separation, which decreases sharply as temperature increases. At high temperature, physical adsorption becomes negligible and permeation is mainly controlled by diffusion [63, 76]. Additionally, due to the fact that CO_2 and N_2 molecules have similar sizes (Table 1), the difference in diffusivity is not a strong controlling factor in determining selectivity.

Modified γ-Al_2O_3 mesoporous membranes have been also reported as a means for CO_2 separation [64]. Transport mechanisms in porous membranes have the contribution of different regimes. An overview of the different mechanisms is given in Table 2.

http://dx.doi.org/10.5772/57444

Transport Type	Pore diameter	Characteristics
Viscous flow	>20 μm	Non selective. Affects the total flow resistance of the membrane system.
Molecular diffusion	>10 μm	
Knudsen diffusion	2 – 100 nm	Occurs when the mean free path of the molecule is much larger than pore radius of the membrane. Shows selectivity based on molecular weights.
Surface diffusion		Shows selectivity due to interaction of molecules with membrane walls.
Capillary condensation		
Micropore diffusion (Configurational diffusion)	< 1.5 nm	

Table 2. Transport mechanisms in porous membranes.

Depending on the particular system, permeability of a membrane can involve several transport mechanisms that take place simultaneously. Considering no membrane defects and pore sizes in the range of 2.5-5 nm, γ-Al_2O_3 based membranes theoretically have two transport regimes: Knudsen diffusion and surface diffusion. Eq. (7) describes the permeability of a membrane by taking into consideration the Knudsen and surface diffusion.

$$F = \left(\frac{2\varepsilon\mu r}{3RTL}\right)\left(\frac{8RT}{\pi M}\right)^{0.5} + \frac{2\varepsilon\mu D_s}{r A_0 N_{av}}\frac{d x_s}{dP} \tag{7}$$

where r is the mean pore radius, μ is a shape factor, R is the universal gas constant, T is the temperature, P is the mean pressure, M is molar mass of the gas, A_o is the surface area occupied by a molecule, D_s is the surface diffusion coefficient, N_{av} is Avogadro's constant and X_s is the percentage of occupied surface compared with a monolayer [81].

For the cases when Knudsen diffusion dominates, selectivity can be correlated to the molecular weights of the permeating gases by the so called Graham's law of diffusion, which establishes that the transport rate of any gas is inversely proportional to the square root of its molecular weight. The CO_2/N_2 separation factor considering pure Knudsen diffusion is given by Eq. (8) and has a value of just 0.8. Therefore, Eq. (8) clearly shows that separation via Knudsen is limited for systems where species are of similar molecular weight.

$$\alpha\left(\frac{CO_2}{N_2}\right) = \sqrt{\frac{M_{CO_2}}{M_{N_2}}} \tag{8}$$

Based on the aforesaid, CO_2/N_2 separation factor can be better enhanced by promoting the surface diffusion mechanism (second term on the right hand side of Eq. (7)). Surface diffusion involves the adsorption of gas molecules on the surface of the pore and subsequent diffusion of the adsorbed species along the surface by a concentration gradient. Then separation

properties of a membrane can be improved by generating such an interaction between one component of the feed gas mixture with the membrane; one option being via a chemical modification.

Cho et al [81] prepared a series of thin (2-5 μm thickness) γ-Al_2O_3 and CaO- or SiO_2-modified γ-Al_2O_3 membranes for CO_2 separation at temperatures between 25 and 400 °C. Impregnation of membranes with SiO_2 or alkaline CaO was done in order to improve the CO_2/N_2 selectivity by promoting adsorption between CO_2 gas molecules and the membrane pore wall. Although this kind of chemical modification of the membrane surface and the pore walls is able to activate the surface diffusion mechanism, an interesting behavior was observed. The CO_2/N_2 separation factor increased from 1.0 to 1.38 at 25 °C after modification of the γ-Al_2O_3 with SiO_2. On the other hand, CaO impregnated membranes showed a separation factor of 0.98, which is even lower than that of the unmodified γ-Al_2O_3. The same behavior has been reported by Uhlhorn et al. [82-83]. They reported MgO modified γ-Al_2O_3 membranes which did not show significant enhancement in the permeation and selectivity properties as a result of the modification process. This fact was explained in terms of the surface diffusion mechanisms. As discussed, it is expected that physicochemical modifications of the membrane can enhance preferential adsorption of the gas species in the feed. Impregnations with alkaline oxide such as calcium oxide or magnesia on the γ-alumina surface give more strong base sites than those promoted by silica. Therefore, it promotes a strong bonding of CO_2 on the alumina surface, causing CO_2 molecules to lose mobility, resulting in a smaller contribution of surface diffusion to the total transport mechanism.

There is another kind of membrane where alkaline and alkaline-earth ceramic oxides have been used for the fabrication of CO_2 permselective membranes. In these cases ceramic materials were chosen because of their well-known properties of physisorption of CO_2 at low and intermediated temperatures.

Kusakabe et al. [84] prepared both pure and modified $BaTiO_3$ CO_2 permselective membranes via the alkoxide based sol-gel method; impregnation and calcination at 600 °C. In order to establish the effects of CO_2 partial pressure, temperature and influence of the secondary oxide presence (CuO, MgO or La_2O) on the CO_2 adsorption properties of the membranes, pure and modified barium titanate powders were first evaluated by thermogravimetry and chromatography techniques. Dynamic CO_2 absorption was evaluated by applying the impulse response method, wherein the $BaTiO_3$ powder was packed in a separation column. The results suggested that the CO_2 molecules adsorbed on the $BaTiO_3$ powder are mobile at temperatures about 500 °C. Therefore, this membrane exhibits CO_2 permeation due to surface diffusion mechanism. Even though the prepared membranes showed selectivity, the Knudsen diffusion still has an important contribution to the gas transport due to the presence of membrane defects. The maximum separation factor of CO_2/N_2 through the membranes was estimated as 1.2. Therefore, further improvement of the permeation properties of this kind of membrane requires obtaining pinhole-free membranes.

Based on the same criteria, Nomura et al. [85] prepared Li_4SiO_4-based thin membranes on porous alumina supports. Membranes were obtained by the thermal treatment of different silica containing porous materials (Silicalite-1 and mesoporous silica) impregnated with

http://dx.doi.org/10.5772/57444

lithium compounds. The authors called this method solid conversion. The use of different silica porous sources was proposed in order to enhance the reaction rate of Si and Li on the porous support at relatively low temperature, avoiding the reaction between the Li and alumina support itself. In the case of Silicalite-1 (MFI zeolite), a zeolite thin film was first prepared on the support by following the dry gel conversion technique. Then, the prepared Silicalite-1 layer was impregnated via dipping into a slurry containing lithium and silica fumed reactants (Li:Si = 4:1) and subsequently into a Li_2CO_3-K_2CO_3 slurry. The membrane was finally calcined at 600 °C for 2 h. It is believed that carbonate melts to fill the cracks and the pinholes of the Li_4SiO_4 formed membrane. A similar procedure of coating and calcination was carried out to prepare high quality membranes starting from mesoporous silica sources with pore sizes of 1.8-12.8 nm. Precursors react to form a Li_4SiO_4 membrane of 2-5 μm thickness that exhibits an N_2 permeance of 1.8 x 10^{-9} mol m^{-2} s^{-1} Pa^{-1} at 400 °C. This suggests there are no big defects after impregnation of the membrane with the binary mixture of Li_2CO_3-K_2CO_3carbonate. Due to the fact that the membrane operates in a rich CO_2 atmosphere, carbonates do not decompose even at temperatures of 600 °C. The maximum CO_2/N_2 permeance ratio was 0.85. The separation factor was higher than that for the Knudsen diffusion. Therefore, it can be conclude that Li_4SiO_4 layer was selective to CO_2 over N_2 at high temperature of 600 °C.

Nomura [86] reported a two -stage approach for the preparation of Li_4SiO_4-CO_2 selective membranes that involves the fabrication of a supported Li_4SiO_4 membrane and its subsequent modification by using a chemical vapor deposition (CVD) method. First, for the preparation of a thin Li_4SiO_4 membrane the so called solid conversion method described before was used, which is based on the reaction between a porous silica source and a lithium containing solution coated on a porous alumina membrane support. Although the formed membranes showed certain selectivity due to the preferential adsorption of CO_2 over N_2, the presence of pinholes and cracks caused low separation factors. Therefore, the membrane defects were fixed by using the counter diffusion CVD method to form a silica coating that fills the gaps between the lithium orthosilicate particles that make up the membrane. N_2 permeance was reduced about three orders of magnitude after CVD modification. Nitrogen permeance before and after the CVD treatment was 3.4 x 10^{-6} mol m^{-2} s^{-1} Pa^{-1} and 1.2 x 10^{-9} mol m^{-2} s^{-1} Pa^{-1} respectively. In the same sense, the CO_2/N_2 permeance rate increased from 0.7 to 1.2 at 600 °C. Some issues related with this system are the chemical and structural stability of the membranes observed during the permeation tests at elevated temperature. The membranes were broken when permeation tests were carried out at temperatures higher than 700 °C, with the consequent decrease in the CO_2/N_2 selectivity. The aforesaid is the result of the CO_2 chemisorption on the membrane. Lithium orthosilicate reacts with CO_2 to form lithium carbonate and lithium metasilicate (Li_2SiO_3) as products, as indicated by Eq. (9).

$$Li_4SiO_4 + CO_2 \longleftrightarrow Li_2CO_3 + Li_2SiO_3 \quad (9)$$

Thermodynamically, this reaction is prone to occur at temperatures between room temperature and about 700 °C. However, experimentally it has been observed that reaction kinetics

sharply increase above 550 °C. At these temperatures, the formation of carbonates involves an important change in volume that ends in the membrane's rupture.

Therefore, one of the issues related to the development of this kind of inorganic membrane is the thermochemical stability. Due to reactivity of alkaline and alkaline-earth ceramic oxides with CO_2 to form carbonates, not only preferential adsorption of CO_2 molecules over N_2 occurs, but CO_2 chemisorption and reaction.. Therefore, it is mandatory to establish the operational temperature within a range where CO_2 selective adsorption on the membrane layer promotes the separation process without reaction.

3.2. Nonporous membranes based on alkaline and alkaline-earth ceramic oxides for CO_2 separation

Some researchers have proposed the use of alkaline and alkaline-earth ceramic oxides to prepare membranes that are able to separate CO_2 at high temperatures via a different transport mechanism than those observed on porous membranes. Li_2ZrO_3 and Li_4SiO_4 based membranes are examples of the aforesaid. Permselectivity of CO_2 through these membranes takes place not only due to the selective CO_2 adsorption properties of ceramic phases but also via a mechanism of gas separation that involves the transport of CO_3^{2-} and O^{2-} ionic species through the electrolytes (carbonate-metal oxide) phases formed by the reaction of the membrane with the CO_2 [87-89].

Kawamura et al. [87] fabricated and characterized a membrane for CO_2 separation at high temperatures. The membrane was made of lithium zirconate (Li_2ZrO_3), an alkaline ceramic oxide that reacts with CO_2 to produced Li_2CO_3 and ZrO_2. These two reaction products are electrolyte materials produced *in-situ* when the membrane is exposed to the rich carbon dioxide atmosphere. The electrolytes formed thus are capable to transport both CO_2 and O_2 across the membrane via a dual ion conduction mechanism. The prepared membrane exhibited a separation factor of 4.9 between CO_2 and CH_4 gas molecules at a temperature of 600 °C. The obtained separation factor is higher than the Knudsen diffusion limit, 0.6. Therefore, the results clearly suggest the potential use of this kind of membrane system for CO_2 separation such as the case of CO_2 removal from natural gas.

Yamaguchi et al. [88] investigated the concept of the dual-ion conduction facilitated mechanism previously observed for the case of Li_2ZrO_3 membranes by focusing their efforts on the preparation of a CO_2 permselective membrane based on lithium orthosilicate (Li_4SiO_4). The supported membrane was prepared via a dip coating technique by using Li_4SiO_4 suspensions. The coating process was repeated several times before impregnation of the membrane with a Li_2CO_3/K_2CO_3 carbonate mixture and final sintering at 750 °C. In this membrane system, Li_4SiO_4 reacts *in-situ* with CO_2 to form Li_2CO_3 and Li_2SiO_3.

Gas separation studies were performed by using CO_2/N_2 mixtures as feed gas. The observed CO_2 permeance values were about 1×10^{-8} mol $m^{-2}s^{-1}Pa^{-1}$ in the temperature range of 525-625 °C. The CO_2/N_2 separation factor was estimated between four and six. Figure 3 shows a scheme of the dual-ion conduction mechanism explained as follows. In the feed side, carbon dioxide dissolves in the material and diffuses as carbonate ions through the molten carbonate electro-

http://dx.doi.org/10.5772/57444

lyte due to a concentration gradient. Then, in the downstream side of the membrane, the formation of gaseous CO_2 implies the formation of oxygen ions which must diffuse back to the feed side across the membrane and apparently through the formed Li_2SiO_3 skeleton to obtain the charge balance.

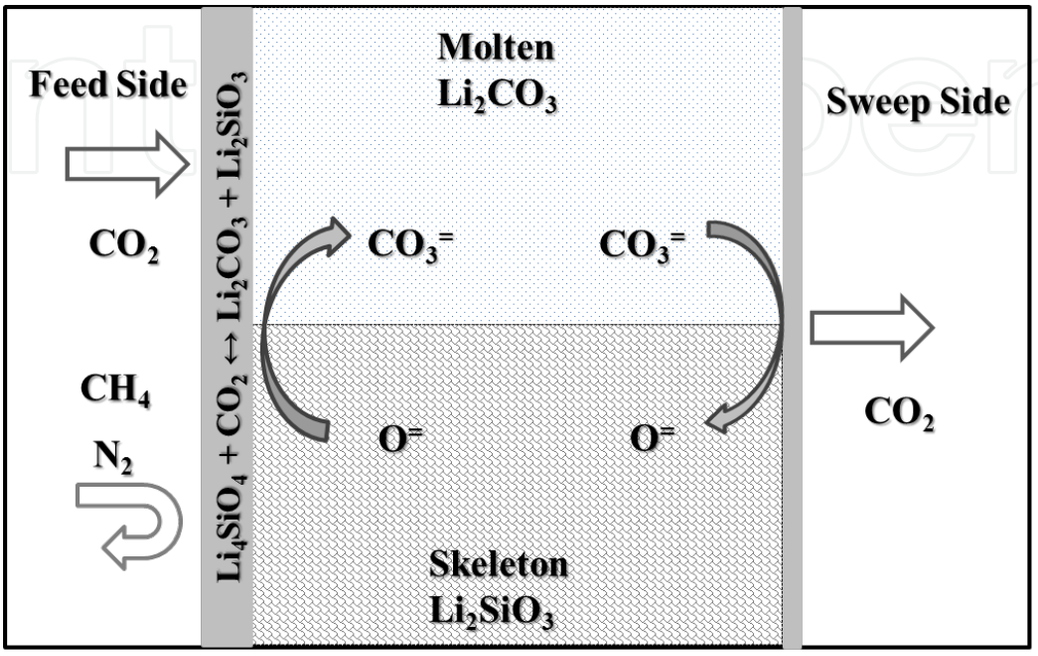

Figure 3. Schematic representation of a membrane system for the CO_2 separation via a dual-ion conduction mechanism.

The proposed transport mechanisms supports the higher selectivity values observed in the permeation test for both systems, Li_2ZrO_3 and Li_4SiO_4. Figure 4 shows the separation factor values (CO_2/N_2) obtained for different ceramic membranes described in the present report. The pure Knudsen value is written as baseline and separation factor of nonporous Li_4SiO_4 for comparison purposes. However, it is important to mention that the oxygen ion diffusion process is not totally clear. Indeed, there is no experimental study regarding the oxygen ionic conductivity properties of Li_2SiO_3 phase. On the other hand, pure ZrO_2 exhibits poor bulk oxygen ion conductivity. In fact, good conduction properties are observed only in acceptor-doped ZrO_2 based materials with oxygen vacancies being the predominant charge carriers [90]. Therefore, oxygen ion conduction through the membrane must be related to different transport paths, such as grain boundaries and interfacial regions formed between the ceramic and molten carbonate on the membrane.

More recently, the promising concept of ceramic oxide-carbonate dual-phase membranes has been proposed for carbon dioxide selective separation at intermediate and high temperatures (450-900 °C) [91-97].

This concept involves the fabrication of nonporous membranes capable of selectively separating CO_2 via its transport, as carbonate ions. Dual phase membranes are made of an oxygen ion

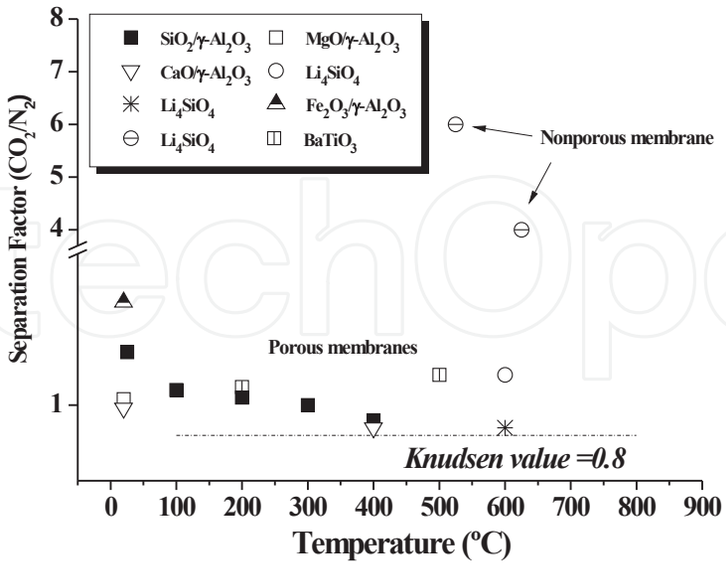

Figure 4. CO_2/N_2 separation factor of different ceramic oxide membranes.

conductive porous ceramic phase that hosts a molten carbonate phase. Rui et al. [98] proposed the CO_2 separation by the electrochemical conversion of CO_2 molecules to carbonate ions (CO_3^{2-}), which are subsequently transported across the membrane. Carbonate ionic species (CO_3^{2-}) are formed by the surface reaction between CO_2 and oxygen that comes from the ceramic oxide phase (feed side, Eq.(10)) and then transport of CO_3^{2-} takes place through the molten carbonate.

$$CO_2 + O_O^{\,x} \longleftrightarrow CO_3^{\,2-} + V_O^{\,\cdot\cdot} \tag{10}$$

Once carbonate ions have reached the permeate side, molecular CO_2 is released to the gas phase, delivering $O_O^{\,x}$ species back to the ceramic oxide solid phase. This process takes place due to a chemical gradient of CO_2 in the system (Figure 5). Here, it is important to emphasize that dual-phase membranes are nonporous and therefore exhibit high separation selectivity as a result of the transport mechanism. Figure 5 also shows the SEM image of the cross section of a ceramic oxide-carbonate membrane prepared by pressing $La_{0.6}Sr_{0.4}Co_{0.8}Fe_{0.2}O_{3-\delta}$ powders and subsequent infiltration of the obtained porous ceramic (bright phase) with carbonate (dark phase).

Table 3 summarizes the different studies reported and certain advances that have been achieved so far regarding the dual-phase membrane concept. This table also includes the Li_2ZrO_3 and Li_4SiO_4 nonporous membranes previously described. Although the original reports do not clearly explain the operational mechanism [26-27], the dual-phase membrane concept gives a much better idea of the possible phenomenology involved [30,33,36].

http://dx.doi.org/10.5772/57444

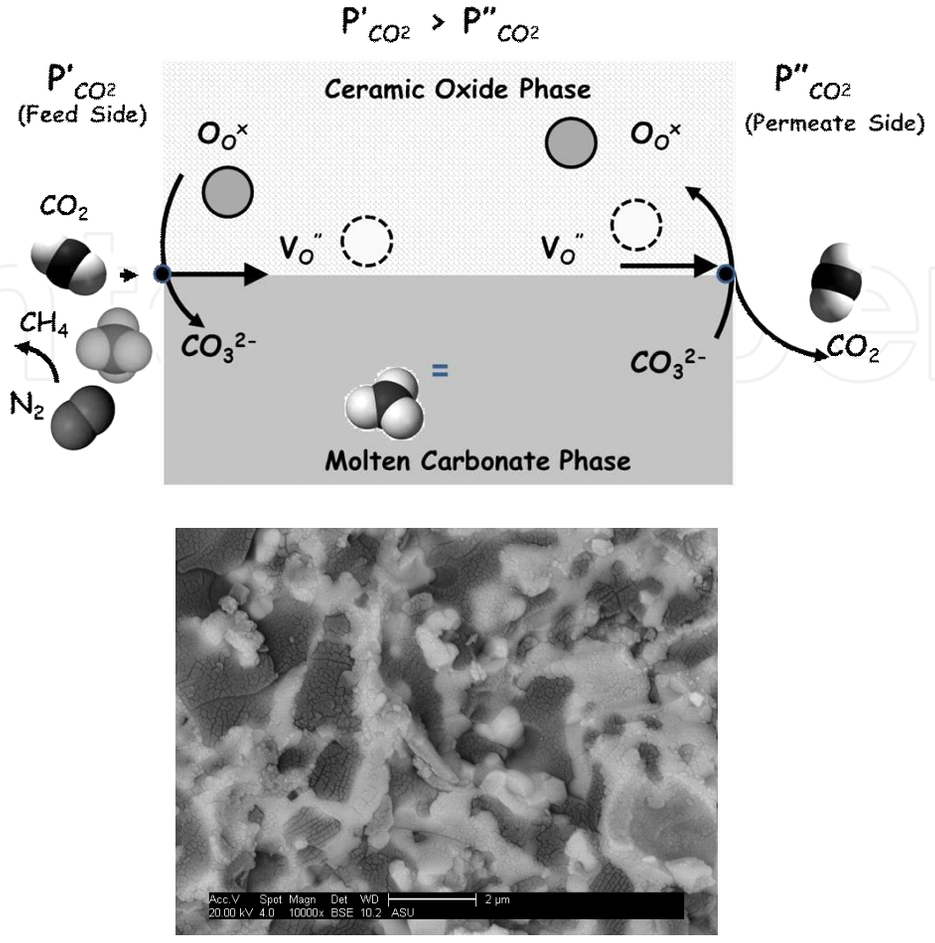

Figure 5. Schematic representation of a membrane system for the CO_2 separation and SEM image of a ceramic oxide-carbonate dual-phase membrane

3.3. Applications of CO_2 permselective ceramic oxide membranes for the design of membrane reactors.

As mentioned, CO_2 can be used as raw material for the synthesis of several chemicals [99]. Moreover, if CO_2 is concentrated or separated by a membrane system exhibiting high CO_2 permeation and permselectivity, this open up the possibility to develop a continuous process of membrane reaction to simultaneously capture and chemically convert CO_2. For example, if the membrane is able to separate CO_2 at intermediate and even high temperatures, it can be used for the design of a membrane reactor for the production and purification of hydrogen and syngas. Syngas is a gaseous fuel with a main chemical composition of CO, H_2, CO_2, and CH_4. Syngas can be used as feedstock for the synthesis of several other clean fuels such as H_2, methanol, ethanol, diesel and other hydrocarbons synthesized via the Fischer-Tropsch process [100-104].

Among the different processes for the synthesis of syngas and hydrogen, CO_2 methane reforming Eq. (11) and the water-gas shift reaction (WGS) Eq. (12) are the most promising options.

Ceramic Oxide phase	Molten Carbonate phase	Membrane features	Preparation method	Permeance (mol.s.$^{-1}$m.$^{-2}$Pa.$^{-1}$)	Separation Factor (CO_2/N_2)	Ref.
Li_2ZrO_3	Li_2CO_3	Thick membrane	*In situ* by exposing Li_2ZrO_3 to CO_2 atmosphere	1 x10^{-8}	4.9 (CO_2/CH_4 at 600°C)	[87]
Li_4SiO_4/Li_2SiO_3	K_2- Li_2CO_3	Thin supported membrane	Impregnation of carbonate	2x10^{-8}	5.5 (at 525°C)	[88]
$La_{0.6}Sr_{0.4}Co_{0.8}Fe_{0.2}O_{3-\delta}$	Li-Na-K_2CO_3	Thick membrane (0.35-1.5 mm)	Pressing and direct infiltration	4.77 x 10^{-8}	225 (at 900°C)	[91]
8 mol% Yttria doped zirconia (YZS) 10 mol% Gadolinia doped ceria (GDC)	Li-Na-K_2CO_3 Li-Na_2CO_3	Thin freestanding membranes (200-400 µm)	Tape casting and in situ infiltration	2.0 x10^{-8} (YSZ) 3.0 x10^{-8} (GDC)	> 2 (at 800 °C)	[92]
$Ce_{0.8}Sm_{0.2}O_{1.9}$	Na_2- Li_2CO_3	Thick membrane (1.2 mm)	Pressing of SDC-NiO powders where NiO is a sacrificial template	~1.2 x 10^{-6}	155-255 (at 700°C)	[93]
$Bi_{1.5}Y_{0.3}Sm_{0.2}O_3$	Li-Na-K_2CO_3	Thin supported membrane (50 µm)	Dip coating of modified thick support and infiltration	1.1 x 10^{-8}	2 (at 650°C)	[94]
8 mol% Yttria doped zirconia (YZS)	Li-Na-K_2CO_3	Thin supported membrane (10 µm)	Dip coating of YSZ on nonwettable thick support and infiltration	~ 7.8×10^{-8}	---	[95]
$Ce_{0.8}Sm_{0.2}O_{1.9}$	Li-Na-K_2CO_3	Thin tubular membrane	Centrifugal casting and direct infiltration			[96]
$La_{0.6}Sr_{0.4}Co_{0.8}Fe_{0.2}O_{3-\delta}$	Li-Na-K_2CO_3	Thick disk-shaped membrane	Pressing and direct infiltration			[97]

Table 3. Reported studies on dual-phase and related membranes for CO_2 separation.

$$CH_4 + CO_2 \longleftrightarrow 2CO + 2H_2 \quad (11)$$

$$CO + H_2O \longleftrightarrow CO_2 + H_2 \quad (12)$$

Figure 6 schematizes the membrane reactor concept considering the two reactions described above. Figure 6A shows a membrane reactor for dry reforming of methane to produce syngas at temperatures between 700 and 800 °C. Figure 6B illustrates the use of ceramic oxide

http://dx.doi.org/10.5772/57444

membranes for hydrogen purification by separating the CO_2 from water-gas shift products at about 550 °C. Additionally, Figure 6B shows the possibility of using a ceramic sorbent to chemically trap the permeate CO_2 and therefore enhance the CO_2 permeation process by reducing the concentration of CO_2 in the permeate side.

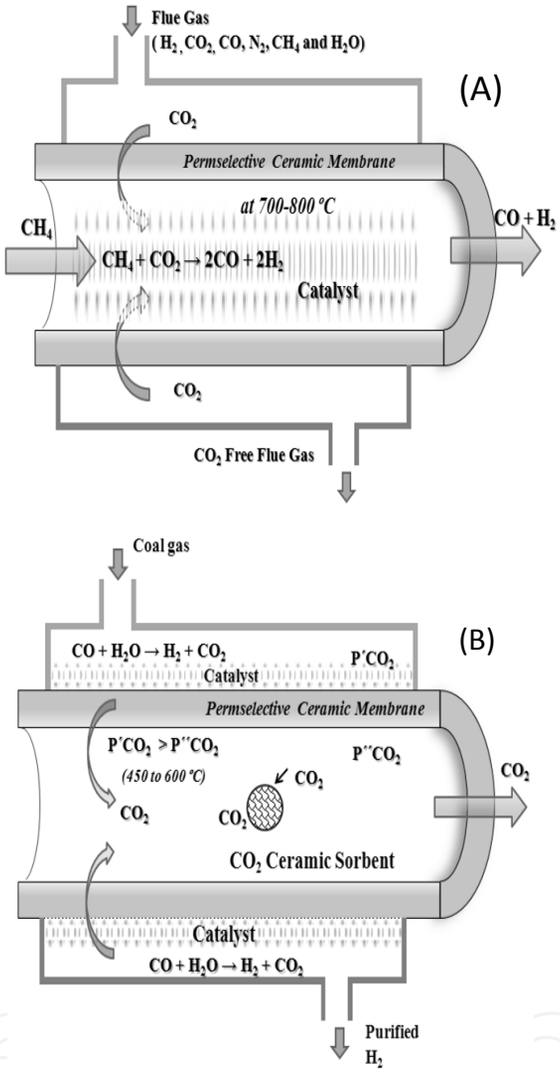

Figure 6. Schematic representation of the membrane reactor concept using a CO_2 permselective ceramic membrane: (a) CO_2 dry methane reforming and (b) water-gas shift reaction with hydrogen purification wherein CO_2 capture promotes the separation process.

4. Chemical transformation of CO_2 catalyzed by ceramic materials: the use of new alternatives.

One of the most widely used chemical absorption techniques for carbon capture and storage/sequestration (CCS) is CO_2 adsorption by ceramic materials. Once CO_2 has been captured-

fixed, it can be converted into value-added products such as precursors in chemical transformation reactions. CO_2 is extensively used for enhanced oil recovery, as a monomer feedstock for urea and polymer synthesis, in the food and beverage industry as a propellant, and in production of chemicals. Therefore, the capture-fixation of CO_2 would make a system suitable for accomplishing chemical transformation of CO_2. The utilization of carbon dioxide is also very attractive because it is environmentally benign [105-115]. CO_2 conversion to fuel and value-added products is an ideal route for CO_2 utilization due to the simultaneous disposal of CO_2 and the benefit that many products can be used as alternate transportation fuels [116]. CO_2 chemical transformation methods include (i) reverse water-gas shift, (ii) hydrogenation to hydrocarbons, alcohols, dimethyl ether and formic acid, (iii) reaction with hydrocarbons to syngas, (iv) photo- and electrochemical/catalytic conversion, and (v) thermo-chemical conversion [100-122].

CO_2 can be catalyzed to valuable organic or inorganic compounds, where some basic catalytic materials (containing alkaline or alkaline-earth elements) are used. The activation of CO_2 by alkali metals has received considerable attention in various surface science studies, which have demonstrated the formation of intermediate CO_2, dissociation of CO_2 and formation of oxalate and carbonate alkali compounds [118-121]. Carbon dioxide has been identified as one such potential vector molecule (through reduction to syngas, methanol, methane, formic acid, formaldehyde, dimethylether (DME) and short-chain olefins) [117-118, 120-122]. CO_2 is a kinetically and thermodynamically stable molecule, so CO_2 conversion reactions are endothermic and need efficient catalysts to obtain high yield. CO_2 conversion to carbon monoxide (CO) looks like the simplest route for CO_2 reduction [121]. CO is a feedstock or intermediate product for the production of methanol and hydrocarbon fuels via Fischer-Tropsch synthesis of CH_4/CO_2 reforming to form syngas (CO/H_2) [122]. CO_2 reforming with CH_4 is an example of CO_2 being used as a soft oxidant, where the dioxide is dissociated into CO and surface oxygen, and oxygen abstracts hydrogen from methane to form water via the water-gas shift reaction (WGS) (Eqs. 11 and 12) [100-103, 121]. The catalytic chemistry of the reverse water-gas shift reaction and the following transformation to methanol/DME (or hydrocarbons via Fischer-Tropsch synthesis), and the subsequent production of gasoline (methanol-to-gasoline or diesel via hydrocracking of the alkanes produced in the Fisher-Tropsch process) are well established [102, 117-122]. On the other hand, methanol can be produced directly from carbon dioxide sources by catalytic hydrogenation and photo-assisted electrochemical reduction. A wide variety of CO_2 photo-reduction methods have been performed to oxygenate products, including formic acid (HCOOH) and formaldehyde (HCHO). HCOOH and HCHO are the simplest oxygenates produced from the reduction of CO_2 with H_2O (or proton solvents) [121]. Furthermore, CO_2 can be utilized as a monomeric building block to synthesize various value-added oxygen-rich compounds and polymers under mild conditions. As an example, chemical conversion of CO_2 through C–N bond formation can produce value-added chemicals such as oxazolidinones, quinazolines, carbamates, isocyanates and polyurethanes [105]. These commodity chemicals have been synthesized from green methods and have important applications in the pharmaceutical and plastic industries. The chemisorption of CO_2 based on C–N bond formation could be one of the most efficient strategies, utilizing liquid absorbents such as conventional aqueous amine solutions, chilled ammonia, amino-functionalized ionic

http://dx.doi.org/10.5772/57444

liquids, and solid absorbents including amino-functionalized silica, carbon, polymers and resins. The processes by which chemicals for CO_2 capture are manufactured should also be considered in terms of their energy requirements, efficiencies, waste products, and CO_2 emissions [105, 123]. In that sense, dimethyl carbonate (DMC) is a promising target molecule derived from CO_2 catalyzed by inorganic dehydrating agents such as molecular sieves [107]. Dimethyl carbonate has received much attention as a safe, non-corrosive, and environmentally friendly building block for the production of polycarbonates and other chemicals, an additive to fuel oil owing to its high octane number and an electrolyte in lithium batteries due to its high dielectric constant. It can be synthesized through a two-step transesterification process utilizing CO_2 as raw material [105, 107].

As a complementary technology to carbon sequestration and storage (CSS), the chemical recycling of carbon dioxide to fuels is an interesting opportunity. Chemical compounds such as alkane products ($C_nH_{(2n+2)}$) are un-branched hydrocarbons suitable for diesel fuel and jet fuel [121]. In this regard, biofuels or biodiesel, catalyzed using ceramic materials, can provide a significant contribution in energy independence and mitigation of climate change [109-127]. Today the main renewable biofuels are bioethanol and biodiesel. Biodiesel is a liquid fuel consisting of mono alkyl esters (methyl or ethyl) of long-chain fatty acids derived from vegetable oils, animal fats or micro and macro algal oils [127]. Biodiesel is a sustainable, renewable, non-toxic, biodegradable diesel fuel substitute that can be employed in current diesel engines without major modification, offering an interesting alternative to petroleum-based diesel [106, 111-115, 124-128]. Besides this, it is free from sulfur and aromatic components, making it cleaner burning than petroleum diesel. Biodiesel has a high flash point, better viscosity and caloric power similar to fossil fuels. It can be mixed with petroleum fossil fuel at any weight ratio or percentage, and it can be used without blending with fossil fuel (B100) as a successful fuel [127, 128]. It has similar properties (physical and chemical) to petroleum diesel fuel. Recently, transesterification (also called alcoholysis) has been reported as the most common way to produce biodiesel with lipid feedstock (such as vegetable oil or algal oil) and alcohol (usually methanol or ethanol), in presence of an acid or base catalyst. Transesterification is the best method for producing higher-quality biodiesel and glycerol [108, 110-115, 124-132]. The reaction is facilitated with a suitable catalyst [129-131]. The catalyst presence is necessary to increase both, the reaction rate and the transesterification reaction conversion yield. The catalysts are classified as homogeneous or heterogeneous. Homogeneous catalysts act in the same liquid phase as the reaction mixture. Conversely, if the catalyst remains in a different phase, the process is called heterogeneous catalytic transesterification [113, 127-131]. Heterogeneous catalysts are mostly applied in transesterification reaction due to many advantages such as easy catalyst separation and reusability, improved selectivity, fewer process stages, no water formation or saponification reaction, including in green technology, and cost effectiveness [127, 132]. The heterogeneous catalysts increase the mass transfer rate during the transesterification reaction [127, 131]. Various ceramic materials have been investigated for the production of biodiesel [106, 109-115, 124-179]. Some of these solid catalysts include alkali and alkaline-earth metal carbonates and oxides such as magnesium oxide (MgO), calcium oxide (CaO), barium oxide (BaO), strontium oxide (SrO) [124-131, 133-143]; lithium base ceramics (Li_4SiO_4 and Li_2SiO_3 [144-146]); sodium silicate (Na_2SiO_3 [147]);

transition metal oxides and derivatives (titanium oxide, zinc oxide, mixed oxides catalysts [148-149]); ion exchange resin type acid heterogeneous catalysts [150]; MCM-metal impregnated materials [114]; layered double hydroxides (hydrotalcite-like hydroxides) [151-154]; hydrocalumite-like compounds [110,155]; supported bases [156-163]; and zeolites [164-165].

Among the alkaline earth metal oxides, CaO is a promising basic heterogeneous catalyst for synthesizing biodiesel at mild temperatures (below the boiling point of methanol, MeOH) and at atmospheric pressure due to its plentiful availability and low cost, but it is rapidly hydrated and carbonated upon contact with room temperature air. CaO is the most widely used catalyst for transesterification and produces a high yield of 98% of fatty acid methyl esters (FAME) during the first cycle of reaction [130]. Granados et al. [142] used activated CaO as a solid base catalyst in the transesterification of sunflower oil to investigate the role of water and carbon dioxide on the deterioration of the catalytic performance upon contact with air for different periods. The study showed that CaO was rapidly hydrated and carbonated in air. Consequently, the reusability of the catalyst for subsequent steps is a big question mark. Di Serio et al. [170] reported a 92% biodiesel yield with MgO catalyst, using 12:1 methanol to oil molar ratio with 5.0wt% of the catalyst at methanol supercritical condition for 1 h. Wen et al. [171] carried out transesterification from waste cooking oil with methanol at 170 °C for 6 h with 10wt % of MgO/TiO_2 and 50:1 M ratio of MeOH and oil. Guo et al. [172] studied the methyl ester yield produced via transesterification of soybean oil using sodium silicate as a catalyst. Sodium silicate was an effective catalyst for the microwave-irradiated production of biodiesel and hydrothermal production of hydrogen from by-product glycerol combined with Ni catalyst. The optimum reaction conditions obtained were 7.5:1 M ratio of alcohol/oil, 3wt% catalyst amount, 1 h reaction time and 60 °C reaction temperature. The FAME yield was ~100%. On the other hand, microwave-assisted transesterification of vegetable oil with sodium silicate is an effective and economical method for the rapid production of biodiesel. The reused catalyst after transesterification process for four cycles was recovered. Overall, sodium silicate was fully used in biodiesel production and glycerol gasification, and this co-production process provided a novel green method for biodiesel production and glycerol utilization [172].

Several techniques have been investigated for the transesterification reaction using heterogeneous catalysts for biodiesel production, as follows: transesterification via radio frequency microwaves, alcohol reflex temperature, alcohol supercritical temperature and ultrasonication [127, 173-177]. Recently, the use of ultrasonic irradiation has gained interest in biodiesel production [173-177]. Ultrasonic energy can emulsify the reactants to reduce the catalyst requirement, methanol-oil ratio, reaction time and reaction temperature and also provides the mechanical energy for mixing and the required activation energy for initiating the transesterification reaction [173-176]. The ultrasound phenomenon has its own physical and chemical effects on the liquid-liquid heterogeneous reaction system through cavitation bubbles, according to the following principles [175]: (1) the chemical effect, in which radicals such as H^+ and OH^- are produced during a transient implosive collapse of bubbles (in a liquid irradiated with ultrasound), which accelerates chemical reaction in the bulk medium; and (2) the physical effect of emulsification, in which the microturbulence generated due to radial motion of bubbles leads to intimate mixing (homogenizing the mixture) of the immiscible reactants.

http://dx.doi.org/10.5772/57444

Accordingly, the interfacial region between the oil and alcohol increases sharply, resulting in faster reaction kinetics and higher conversion of oil and biodiesel yield [127]. In 2000, the ultrasonication reactor was first introduced by Hielscher Ultrasonic GmbH for biodiesel production. Nishimura et al. [175] studied the transesterification of vegetable oil using low-frequency ultrasound (28-40kHz). An excellent yield (~98%) was obtained at a 28 kHz ultrasound while a significant reduction of reaction time was obtained by using 40 kHz ultrasound. Salamatinia et al. [176] used ultrasonic assisted transesterification to improve the reaction rate. In this study, they used SrO and BaO as heterogeneous catalysts in the production of biodiesel from palm oil. The results showed that the basic properties of the catalyst were the main cause for their high activity. The low-frequency ultrasonic assisted transesterification process had no significant mechanical effects on SrO, but BaO catalyst study confirmed that the ultrasound treatment significantly improved the process by reducing the reaction time to less than 50 min at a catalyst loading of 2.8wt% to achieve biodiesel yield higher than 95%. Another study of alkali earth metals was carried out by Mootabadi et al. [177]. They reported the effect of ultrasonic waves at 20 kHz and 200W on the regenerated catalyst and compared mechanical stirring and ultrasonic irradiation. They investigated the optimum conditions, using palm oil for biodiesel production with catalysts such as CaO, SrO and BaO. They concluded that catalyst leaching was the main cause for the catalyst inactivity in the case of the re-used catalyst. BaO catalyst was found to be stable during the leaching. At the optimized condition, 95.2% yield was achieved with 60 min of reaction time for both BaO and SrO catalysts. For CaO catalyst, 77.3% yield was achieved with the same conditions. The use of ultrasound showed great enhancement of the reaction parameters in terms of the obtained yield and reaction time. The obtained yields were 30 to 40% higher in comparison to the corresponding results obtained using a conventional stirring reactor system without ultrasonication. Deng et al. [178] prepared nano-sized mixed Mg/Al oxides. Due to their strong basicity, the nanoparticles were further used as catalyst for biodiesel production from jatropha oil. Experiments were conducted with the solid basic catalyst in an ultrasonic transesterification reaction. Under the optimum conditions, biodiesel yield was 95.2%. After removing the glycerol on the catalyst surface, the nano-sized mixed Mg/Al oxides were reused eight times. The authors concluded that calcination of hydrotalcite nanocatalyst under ultrasonic radiation is an effective method for the production of biodiesel from jatropha oil. The activity of base solid catalysts is associated to their basic strength, such that the most basic catalyst showed the highest conversion. In another work, Deng et al. [179] reported optimum conditions for biodiesel production in the presence of base solid catalysts. They studied BaO and Ca–Mg–Al hydrotalcite (the most effective). The 95% biodiesel yield from jatropha oils and Ca–Mg–Al hydrotalcite was established with 30 min of reaction time. Ca–Mg–Al hydrotalcite could be reused twelve times after washing of the adsorbed glycerol from the catalyst surface with ethanol. Other types of heterogeneous catalysts under ultrasonic irradiation were used for transesterification by Georgogianni et al. [114]. They studied a wide range of catalysts including Mg-MCM-41, Mg–Al hydrotalcite and K^+-impregnated zirconium oxide. They mixed frying oils, methanol and the catalyst in a batch reactor with mechanical stirring for 24 h and with ultrasonication for 5 h. The results suggested that the basic strength was the cause of the good activity of the catalysts. Mg–Al hydrotalcite achieved the highest reaction conversion of 87% at a reaction temperature of 60 °C. Overall,

ultrasonic irradiation significantly enhanced the reaction rate, causing a reduction in reaction time, and the biodiesel yield increased [114]. Consequently, a better understanding of the use of ultrasonic sound waves to accelerate the transesterification process could lead to substantial future improvement of both batch and continuous production systems, to obtain a more sustainable biodiesel production process [127].

Author details

Margarita J. Ramírez-Moreno[1,2], Issis C. Romero-Ibarra[1], José Ortiz-Landeros[2] and Heriberto Pfeiffer[1*]

*Address all correspondence to: pfeiffer@iim.unam.mx

1 Instituto de Investigaciones en Materiales, Universidad Nacional Autónoma de México, Circuito exterior s/n, Ciudad Universitaria, Del. Coyoacán, México DF, Mexico

2 Departamento de Ingeniería en Metalurgia y Materiales, Escuela Superior de Ingeniería Química e Industrias Extractivas, IPN, UPALM, México DF, Mexico

References

[1] Ortiz-Landeros J.; Ávalos-Rendón T. L.; Gómez-Yáñez C.; Pfeiffer H. *Analysis and Perspectives Concerning CO_2 Chemisorption on Lithium Ceramics Using Thermal Analysis.* J. Therm. Anal. Calorim. 2012, 108, 647–655.

[2] Ávalos-Rendón T.; Casa-Madrid J.; Pfeiffer H. *Thermochemical Capture of Carbon Dioxide on Lithium Aluminates ($LiAlO_2$ and Li_5AlO_4): A New Option for the CO_2 Absorption.* J. Phys. Chem. A 2009, 113, 6919–6923.

[3] Mejia-Trejo V. L.; Fregoso-Israel E.; Pfeiffer H. *Textural, Structural, and CO_2 Chemisorption Effects Produced on the Lithium Orthosilicate by Its Doping with Sodium ($Li_{4-x}Na_xSiO_4$).* Chem. Mater. 2008, 20, 7171–7176.

[4] Mosqueda H. A.; Vazquez C.; Bosch P.; Pfeiffer H. *Chemical Sorption of Carbon Dioxide (CO_2) on Lithium Oxide (Li_2O).* Chem. Mater. 2006, 18, 2307–2310.

[5] Shan S. Y.; Jia Q. M.; Jiang L. H.; Li Q. C.; Wang Y. M.; Peng J. H. *Novel Li_4SiO_4-Based Sorbents from Diatomite for High Temperature CO_2 Capture.* Ceram. Int. 2013, 39, 5437–5441.

[6] Olivares-Marín M.; Castro-Díaz M.; Drage T. C.; Maroto-Valer M. M. *Use of Small-Amplitude Oscillatory Shear Rheometry to Study the Flow Properties of Pure and Potassi-*

um-Doped Li_2ZrO_3 Sorbents During the Sorption of CO_2 at High Temperatures. Sep. Purif. Technol. 2010, 73, 415–420.

[7] Pacciani R.; Torres J.; Solsona P.; Coe C.; Quinn R.; Hufton J.; Golden T.; Vega L. F. *Influence of the Concentration of CO_2 and SO_2 on the Absorption of CO_2 by a Lithium Orthosilicate-Based Absorbent*. Environ. Sci. Technol. 2011, 45, 7083–7088.

[8] Xiao Q.; Tang X.; Liu Y.; Zhong Y.; Zhu W. *Citrate Route to Prepare K-Doped Li_2ZrO_3 Sorbents with Excellent CO_2 Capture Properties.* Chem. Eng. J. 2011, 174, 231–235.

[9] Xiao Q.; Liu Y.; Zhong Y.; Zhu W. *A Citrate Sol-Gel Method to Synthesize Li_2ZrO_3 Nanocrystals with Improved CO_2 Capture Properties*. J. Mater. Chem. 2011, 21, 3838–3842.

[10] Rodríguez-Mosqueda R.; Pfeiffer H. *Thermokinetic Analysis of the CO_2 Chemisorption on Li_4SiO_4 by Using Different Gas Flow Rates and Particle Sizes*. J. Phys. Chem. A 2010, 114, 4535–4541.

[11] Ortiz-Landeros J.; Gomez-Yañez C.; Palacios-Romero L. M.; Lima E.; Pfeiffer H. *Structural and Thermochemical Chemisorption of CO_2 on $Li_{4+x}(Si_{1-x}Al_x)O_4$ and $Li_{4-x}(Si_{1-x}V_x)O_4$ Solid Solutions*. J. Phys. Chem. A 2012, 116, 3163–3171.

[12] Alcerreca-Corte I.; Fregoso-Israel E.; Pfeiffer H. *CO_2 Absorption on Na_2ZrO_3: A Kinetic Analysis of the Chemisorption and Diffusion Processes*. J. Phys. Chem. C 2008, 112, 6520–6525.

[13] Pfeiffer H.; Vazquez C.; Lara V. H.; Bosch P. *Thermal Behavior and CO_2 Absorption of $Li_{2-x}Na_xZrO_3$ Solid Solutions.* Chem. Mater. 2007, 19, 922–926.

[14] Zhao T.; Ochoa-Fernández E.; Rønning M.; Chen D. *Preparation and High-Temperature CO_2 Capture Properties of Nanocrystalline Na_2ZrO_3*. Chem. Mater. 2007, 19, 3294–3301.

[15] Seggiani M.; Puccini M.; Vitolo S. *Alkali Promoted Lithium Orthosilicate for CO_2 Capture at High Temperature and Low Concentration.* Int. J. Greenhouse Gas Control 2013, 17, 25–31.

[16] Khokhani M.; Khomane R. B.; Kulkarni B. D. *Sodium-Doped Lithium Zirconate Nano-Squares: Synthesis, Characterization and Applications for CO_2 Sequestration*. J. Sol-Gel Sci. Technol. 2012, 61, 316–320.

[17] Veliz-Enriquez M. Y.; Gonzalez G.; Pfeiffer H. *Synthesis and CO_2 Capture Evaluation of $Li_{2-x}K_xZrO_3$ Solid Solutions and Crystal Structure of a New Lithium-Potassium Zirconate Phase*. J. Solid State Chem. 2007, 180, 2485–2492.

[18] Martínez-dlCruz L.; Pfeiffer H. *Microstructural Thermal Evolution of the Na_2CO_3 Phase Produced During a Na_2ZrO_3–CO_2 Chemisorption Process*. J. Phys. Chem. 2012, 116, 9675–9680.

[19] Santillan-Reyes G. G.; Pfeiffer H. *Analysis of the CO_2 Capture in Sodium Zirconate (Na_2ZrO_3). Effect of the Water Vapor Addition*. Int. J. Greenhouse Gas Control 2011, 5, 1624–1629.

[20] Iwana A.; Stephenson H.; Ketchie C.; Lapkin A. *High Temperature Sequestration of CO_2 Using Lithium Zirconates*. Chem. Eng. J. 2009, 146, 249–258.

[21] Tabarés F. L. Editor, *Lithium: Technology, Performance and Safety*, Nova Publishers, (2013). Chapter 6, *Lithium Ceramics as an Alternative for the CO_2 Capture. Analysis of Different Physicochemical Factors Controlling this Process*, pp 171-192.

[22] Bish D.L., *Anion-Exchange in Takovite: Applications to Other Hydroxide Minerals*, Bone Miner., 1980, 103, 170-175.

[23] Duan X.; Evans D. G., *Layered Double Hydroxides. Structure and Bonding*, Eds. Springer-Verlag: Berlin Heidelberg. Germany, 2006; vol. 119.

[24] Wang M. Z.; Hu Q. D. L.; Li Y.; Li S.; Zhang X.; Xi M.; Yang X., *Intercalation of Ga^{3+}-Salicylidene-Amino Acid Schiff Base Complexes into Layered Double Hydroxides: Synthesis, Characterization, Acid Resistant Property, in Vitro Release Kinetics and Antimicrobial Activity*, Appl. Clay Sci. 2013, 83&84, 182-190.

[25] Catti M.; Ferraris G.; Hull S.; Pavese A. *Static Compression and H Disorder in $Mg(OH)_2$ (Brucite) to 11 GPa: a Powder Neutron Diffraction Study*. Phys. Chem. Miner. 1995, 22, 200-206.

[26] He J.; Wei M.; Li B.; Kang Y.; Evans D. G.; Duan X., *Preparation of Layered Double Hydroxides,* Structure and Bonding, 2005, 119, 89-119.

[27] Gutmann N.; Müller B. *Insertion of the Dinuclear Dihydroxo-Bridged Cr(III) Aquo Complex into the Layered Double Hydroxides of Hydrotalcite-Type*. J. Solid State Chem. 1996, 122, 214-220.

[28] Fogg A.M.; Williams G.R.; Chester R.; O'Hare D. *A Novel Family of Layered Double Hydroxides—$[MgAl_4(OH)_{12}]$ $(NO_3)_2$ xH_2O (M = Co, Ni, Cu, Zn)*. J. Mater. Chem., 2004, 14, 2369-2371.

[29] de Roy A.; Forano C.; Besse J.P. *Layered Double Hydroxides: Synthesis and Post-Synthesis Modification*. Review, Chapter 1, 2002.

[30] Choi S.; Drese J.H.; Jones C.W. *Adsorbent Materials for Carbon Dioxide Capture from Large Anthropogenic Point Sources*. ChemSusChem. 2009, 2, 796-854.

[31] Ding Y.; Alpay, E. *Equilibria and Kinetics of CO_2 Adsorption on Hydrotalcite Adsorbent*. Chem. Eng. Sci. 2000, 55, 3461-3474.

[32] Reijers H.T.J.; Valster-Schiermeier S.E.A.; Cobden P.D.; van der Brink R.W. *Hydrotalcite as CO_2 Sorbent for Sorption-Enhanced Steam Reforming of Methane*. Ind. Eng. Chem. Res. 2006, 45, 2522-2530.

[33] Wang X.P.; Yu J.J.; Cheng J.; Hao Z.P.; Xu Z.P. *High Temperature Adsorption of Carbon Dioxide on Mixed Oxides Derived from Hydrotalcite-Like Compounds*. Environ. Sci. Technol. 2008, 42, 614-618.

[34] Reynolds S.P.; Ebner A.D.; Ritter J.A. *Carbon Dioxide Capture from Flue Gas by Pressure Swing Adsorption at High Temperature Using a K-Promoted HTLC: Effects of Mass Transfer on the Process Performance*. Environ. Prog. 2006, 25, 334-342.

[35] Reynolds, S.P.; Ebner, A.D.; Ritter, J.A. *Stripping PSA Cycles for CO_2 Recovery from Flue Gas at High Temperature Using a Hydrotalcite Like Adsorbent*. Ind. Eng. Chem. Res. 2006, 45, 4278-4294.

[36] Ebner, A.D.; Reynolds, S.P.; Ritter, J.A. *Nonequilibrium Kinetic Model that Describes the Reversible Adsorption and Desorption Behavior of CO_2 in a K-Promoted Hydrotalcite-Like Compound*. Ind. Eng. Chem. Res. 2007, 46, 1737-1744.

[37] Cavani F.; Trifirb F.; Vaccari A. *Hydrotalcite-Type Anionic Clays: Preparation, Properties and Applications*, Catal. Today, 1991, 11, 173–301.

[38] Vaccari A. *Preparation and Catalytic Properties of Cationic and Anionic Clays*, Catal. Today, 1998, 41, 53–71.

[39] Das N.N.; Konar J.; Mohanta M.K.; Srivastava S.C. *Adsorption of Cr(VI) and Se(IV) from their Aqueous Solutions onto Zr^{4+}-Substituted ZnAl/MgAl-Layered Double Hydroxides: Effect of Zr^{4+} Substitution in the Layer*, J. Colloid Interf. Sci., 2004, 270, 1–8.

[40] Goh K.H.; Lim T.T; Dong Z. *Application of Layered Double Hydroxides for Removal of Oxyanions: A Review*, Water Research, 2008, 42, 1343–1368.

[41] Yong Z.; Mata, V.; Rodriguez, A.E. *Adsorption of Carbon Dioxide onto Hydrotalcite-Like Compounds (HTLCs) at High Temperatures*. Ind. Eng. Chem. Res. 2001, 40, 204-209.

[42] Bellotto M.; Rebours B.; Clause O.; Lynch J.; Bazin D.; Elkaîm E. *Hydrotalcite Decomposition Mechanism: A Clue to the Structure and Reactivity of Spinel-Like Mixed Oxides*, J. Phys. Chem. 1996, 100, 8535-8542.

[43] Ram Reddy M. K., Xu Z. P., Lu G. Q. (Max); Diniz da Costa J. C. *Layered Double Hydroxides for CO_2 Capture: Structure Evolution And Regeneration*. Ind. Eng. Chem. Res. 2006, 45, 7504-7509.

[44] Hufton J.; Mayorga S.; Gaffeney T.; Nataraj S.; Sircar S. *Sorption Enhanced Reaction Process (SERP),* Proceedings of the 1997 U.S., DOE Hydrogen Program Review, 1997, 1, 179-194.

[45] Ram Reddy M.K.; Xu Z.P.; Lu G.Q. (Max); Diniz da Costa J.C. *Influence of Water on High-Temperature CO_2 Capture Using Layered Double Hydroxide Derivatives*. Ind. Eng. Chem. Res. 2008, 47, 2630-2635.

[46] Martunus; Othman M.R; Fernando W.J.N. *Elevated Temperature Carbon Dioxide Capture Via Reinforced Metal Hydrotalcite.* Micropor. Mesopor. Mater. 2011, 138, 110–117.

[47] Yong Z.; Rodrigues A.E. *Hydrotalcite-Like Compounds as Adsorbents for Carbon Dioxide*. Energy Convers. & Manage. 2002, 43, 1865-1876.

[48] Newman S. P.; Jones W. *Supramolecular Organization and Materials Design*, Cambridge University Press, England, 2001.

[49] Yamamoto T.; Kodama T.; Hasegawa N.; Tsuji M.; Tamura Y. *Synthesis of Hydrotalcite with High Layer Charge for CO_2 Adsorbent*. Energy Convers Mgmt, 1995, 36, 637-640.

[50] Wang Q.; Wu Z.; Tay H. H.; Chen L.; Liu Y.; Chang J.; Zhong Z.; Luo J.; Borgna A. *High Temperature Adsorption of CO_2 on Mg-Al Hydrotalcite: Effect of the Charge Compensating Anions and the Synthesis pH*. Catal. Today, 2011, 164, 198-203

[51] Wang Q.; Tay H.H.; Ng D.J.W.; Chen L.; Liu Y.; Chang J.; Zhong Z.; Luo J.; Borgna A. *The Effect of Trivalent Cations on the Performance of Mg-M-CO_3 Layered Double Hydroxides for High-Temperature CO_2 Capture*. ChemSusChem. 2010, 3, 965-973.

[52] Hibino T.; Yamashita Y.; Kosuge K.; Tsunashima A. *Decarbonation Behavior of Mg-Al-CO_3 Hydrotalcite-Like Compounds During Heat Treatment*,. Clays Clay Minerals. 1995, 43, 427 – 432.

[53] Qian W.; Luo J.; Zhong Z.; Borgna A. *CO_2 Capture by Solid Adsorbents and their Applications: Current Status and New Trends.* Energy Environ. Sci., 2011, 4, 42-55.

[54] Hufton J. R.; Mayorga S.; Sircar S. *Sorption-Enhanced Reaction Process for Hydrogen Production*. AIChE J. 1999, 45, 248.

[55] Oliveira E.L.G.; Grande C.A.; Rodrigues A.E.; *CO_2 Sorption on Hydrotalcite and Alkali-Modified (K and Cs) Hydrotalcites at High Temperatures*. Sep. Purif. Technol. 2008, 62, 137-147.

[56] Yang J. I.; Kim J. N. *Hydrotalcites for Adsorption of CO_2 at High Temperature.* Korean J. Chem. Eng., 2006, 23, 77-80.

[57] Ida J.I.; Lin S. *Mechanism of High-Temperature CO_2 Sorption on Lithium Zirconate*. Environ. Sci. Technol., 2003, 37, 1999-2004.

[58] Hufton J.; Mayorga S.; Nataraj S.; Sircar S.; Rao M. *Sorption-Enhanced Reaction Process (SERP*), Proceedings of the 1998, USDOE Hydrogen Program Review, 1998, 2, 693-705.

[59] Lee Jung M.; Min Yoon J.; Lee Ki B.; Jeon Sang G.; Na Jeong G.; Ryu Ho J. *Enhancement of CO_2 Sorption Uptake on Hydrotalcite by Impregnation with K_2CO_3*. Langmuir, 2010, 26, 18788–18797.

[60] Baker R. W. *Membrane Technology and Applications*, 2nd Editions, John Wiley and Sons (2004).

[61] Murder M., *Basic Principles of Membrane Technology*, Kluwer Academic Publishers (1991).

[62] Aresta M.; Dibenedetto A. *The Contribution of the Utilization Option to Reducing the CO_2 Atmospheric Loading: Research Needed to Overcome Existing Barriers for a Full Exploitation of the Potential of The CO_2 Use*, Cat. Today. 2004, 98, 455–462.

[63] Anderson M.; Wang H.; Lin Y. S. *Inorganic Membranes for Carbon Dioxide and Nitrogen Separation*, Rev. Chem. Eng., 2012, 28, 101-121.

[64] Yang H.; Xu Z.; Fan M.; Gupta R.; Slimane R. B.; Bland A. E.; Wright I. *Progress in Carbon Dioxide Separation and Capture: A Review*, J. Environ. Sci., 2008, 20, 14-27.

[65] Niwa M.; Katada N.; Okumura K. *Introduction to Zeolite Science and Catalysis, Characterization and Design of Zeolite Catalysts*, Springer Series in Materials Science, Vol. 141 (2010).

[66] Iwamoto Y.; Kawamoto H. *Science and Technology Trends: Quarterly Report*, 2009, 32, 42-59.

[67] Algieri C.; Barbieri G.; Drioli E.; *Zeolite Membranes for Gas Separations, in Membrane Engineering for the Treatment of Gases*. Royal Society of Chemistry Vol. 2 (2011).

[68] Fedosov D. A.; Smirnov A. V.; Knyazeva E. E.; Ivanova I. I. *Zeolite membranes: Synthesis, properties, and application*, Petroleum Chem., 2011, 51, 657-667.

[69] Caro J.; Noack M. *Zeolite membranes – Recent developments and progress.* Micropor. Mesopor. Mater. 2008, 115, 215–233.

[70] Jia M. D.; Peinemann K. V.; Behling R. D. *Ceramic Zeolite Composite Membranes. Preparation, Characterization and Gas Permeation*. J. Memb. Sci. 1993, 82, 15-26.

[71] Cui Y.; Kita H.; Okamoto K. I. *Preparation and Gas Separation Performance of Zeolite T Membrane.* J. Mater. Chem. 2004, 14, 924.

[72] Poshusta J.; Tuan V.; Pape E.; Noble R.; Falconer J. *Separation of Light Gas Mixtures Using SAPO-34 Membranes.* AIChE J. 2000, 46, 779-789.

[73] Li S.; Falconer J.; Noble R. *SAPO-34 Membranes for CO_2/CH_4 Separation.* J. Memb. Sci., 2004, 241, 121–135.

[74] Tomita T.; Nakayama K.; Sakai H. *Gas Separation Characteristics of DDR Type Zeolite Membrane.* Micropor. Mesopor. Mater. 2004, 68, 71.

[75] Caro J.; Noack M. *Zeolite Membranes: Recent Developments and Progress.* Micropor. Mesopor. Mater. 2008, 115, 215-233.

[76] Burggraaf A. J. *Fundamentals of Inorganic Membrane Science and Technology, Membrane Science and Technology*, Series, 4, Elsevier Science. Netherlands (1996).

[77] Lara-Medina J. J.; Torres-Rodriguez M.; Gutierrez-Arzaluz M.; Mugica-Alvarez V. *Separation of CO_2 and N_2 with a Lithium-Modified Silicalite-1 Zeolite Membrane.* Inter. J. Greenhouse Gas Control, 2012, 10, 494-500.

[78] Dyer A. *Introduction to Zeolite Science and Practice*. 3rd Revised Edition. J. Cejka, H. van Bekkum, A. Corma and F. Schiith (Editors) Elsevier B.V. (2007).

[79] An W.; Swenson P.; Gupta A.; Wu L.; Kuznicki T. M.; Kuznicki S. M. *Improvement of H_2/CO_2 Selectivity of the Natural Clinoptilolite Membranes by Cation Exchange Modification.* J. Memb. Sci., 2013, 433, 25–31.

[80] White J. C.; Dutta P. K.; Shqau K.; Verweij H. *Synthesis of Ultrathin Zeolite Y Membranes and their Application for Separation of Carbon Dioxide and Nitrogen Gases*. Langmuir 2010, 26, 12, 10287–10293.

[81] Cho Y.K., Han K., Lee K.H. *Separation of CO_2 by Modified γ-Al_2O_3 Membranes at High Temperature.* J. Membrane Sci. 1995, 104, 219-230.

[82] Keizer K.; Uhlhorn R.J.R.; van Vuren R.J.; Burggraaf A.J. *Gas Separation Mechanisms in Microporous Modified γ-$A1_2O_3$ Membranes.* J. Membrane Sci., 1988, 39, 285-300.

[83] Uhlhorn R.J.R.; Keizer K., Burggraaf A.J. *Gas and Surface Diffusion in Modified 33-Alumina Systems.* J. Membrane Sci., 1989, 46, 225-241.

[84] Kusakabe K., Ichiki K., Morooka S. *Separation of CO_2 with $BaTiO_3$ Membrane Prepared by the Sol—Gel Method.* J. Membrane Sci. 1944, 95, 171-177.

[85] Nomura M., Sakanishi T., Nishi Y., Utsumi K., Nakamura R.. *Preparation of CO_2 Permselective Li_4SiO_4 Membranes by Using Mesoporous Silica as a Silica Source.* Energy Procedia 2013, 37, 1004-1011.

[86] Nomura M.; Nishi Y.; Sakanishi T.; Utsumi K.; Nakamura R. *Preparation of Thin Li_4SiO_4 Membranes by Using a CVD Method*, Energy Procedia 2013, 37, 1012-1019.

[87] Kawamura H.; Yamaguchi T.; Nair B. N.; Nakagawa K.; Nakao S.I. *Dual-Ion Conducting Lithium Zirconate-Based Membranes for High Temperature CO_2 Separation.* J. Chem. Eng. Jpn. 2005, 38, (5) 322-328.

[88] Yamaguchi T.; Niitsume T.; Nair B. N.; Nakagawa K. *Lithium Silicate Based Membranes for High Temperature CO_2 Separation.* J. of Membrane Sci., 2007, 294, 16-21.

[89] Nair B.N.; Burwood R.P.; Goh V.J.; Nakagawa K.; Yamaguchi T. *Lithium Based Ceramic Materials and Membranes for High Temperature CO_2 Separation*. Progress in Materials Sci. 2009, 54, 511–541.

[90] Skinner S.J.; Kilner J.A. *Oxygen Ion Conductors.* Materials Today, 2003, 6, 30-37.

[91] Anderson M.; Lin Y.S. *Carbonate–Ceramic Dual-Phase Membrane for Carbon Dioxide Separation*. J. Membrane Sci. 2010, 357, 22.

[92] Wade J. L.; Lee C.; West A. C.; Lackner K. S. *Composite Electrolyte Membranes for High Temperature CO_2 Separation*. J. Membrane Sci. 2011, 369, 20.

[93] Zhang L.; Xu N.; Li X.; Wang S.; Huang K.; Harris W. H.; Wilson K.; Chiu S. *High CO_2 Permeation Flux Enabled by Highly Interconnected Three-Dimensional Ionic Channels in Selective CO_2 Separation Membranes*. Energy Environ. Sci. 2012, 5, 8310.

[94] Rui Z.; Anderson M.; Li Y.; Lin Y.S. *Ionic Conducting Ceramic and Carbonate Dual Phase Membranes for Carbon Dioxide Separation,* J. Membrane Sci. 2012, 417-418, 174.

[95] Lu B.; Lin Y.S. *Synthesis and Characterization of Thin Ceramic-Carbonate Dual-Phase Membranes for Carbon Dioxide Separation.* J. Membrane Sci. 2013, 444, 402–411.

[96] Dong X.; Ortiz-Landeros J.; Lin Y. S. *An Assymetric Thin Tubular Dual Phase Membrane.* Chem. Commun. 2013, 49, 9654.

[97] Ortiz-Landeros J.; Norton T.T.; Lin Y.S. *Effects of Support Pore Structure on Carbon Dioxide Permeation of Ceramic-Carbonate Dual-Phase Membranes.* Chem. Eng. Sci. 2013, 104, 891-898.

[98] Rui Z.; Anderson M.; Lin Y.S.; Li Y.; *Modeling and Analysis of Carbon Dioxide Permeation through Ceramic-Carbonate Dual-Phase Membranes*. J. Membrane Sci. 2009, 345, 110.

[99] Yu K.M.K.; Curcic I.; Gabriel J.; Tsang S.C.E. *Recent Advances in CO_2 Capture and Utilization*, ChemSusChem. 2008, 1, 893–899.

[100] Wender I. *Reactions of Synthesis Gas,* Fuel Process. Technol. 1996, 48, 3, 189-297.

[101] Rostrup-Nielsen J. R. *Syngas in Perspective*. Catal. Today 2002, 71, 3-4, 243-247.

[102] Dry M.E. *The Fischer–Tropsch Process*: *1950–2000.* Catal. Today 2002, 71, 227-241.

[103] Yu K.M.K.; Curcic I.; Gabriel J.; Tsang S.C.E. *Recent Advances in CO_2 Capture and Utilization.* ChemSusChem. 2008, 1, 893 – 899.

[104] Gnanapragasam N.; Reddy B.; Rosen M. *Reducing CO_2 Emissions for an IGCC Power Generation System: Effect of Variations in Gasifier and System Operating Conditions.* Energ. Convers. Manage. 2009, 50, 1915-1923.

[105] Yang Z.Z.; He L.N.; Gao J.; Liu A.H.; Yu B. *Carbon Dioxide Utilization with C–N Bond Formation: Carbon Dioxide Capture and Subsequent Conversion.* Energy Environ. Sci. 2012, 5, 6602-6639.

[106] Chattopadhyay S.; Sen R. *Fuel Properties, Engine Performance and Environmental Benefits of Biodiesel Produced by a Green Process.* Appl. Energ. 2013, 105, 319–326.

[107] Choi J.C.; He L.N.; Yasuda H.; Sakakura T. *Selective and High Yield Synthesis of Dimethyl Carbonate Directly from Carbon Dioxide and Methanol.* Green Chem. 2002, 4, 230–234.

[108] Quispe C.A.; Coronado J.R.C; CarvalhoJr J.A. *Glycerol: Production, Consumption, Prices, Characterization and New Trends in Combustion.* Renew. Sust. Energ. Rev. 2013, 27, 475–493.

[109] Talebian-Kiakalaieh A.; Saidina Amin N. A; Mazaheri H. *A Review on Novel Processes of Biodiesel Production from Waste Cooking Oil.* Appl. Energ. 2013, 104, 683–710.

[110] Kuwahara Y.; Tsuji K.; Ohmichi T.; Kamegawa T.; Moria K.; Yamashita H. *Transesterifications Using a Hydrocalumite Synthesized from Waste Slag: An Economical and Ecological Route for Biofuel Production.* Catal. Sci. Tech. 2012, 2, 1842–1851.

[111] Atadashi I.M.; Aroua M.K.; Abdul Aziz A. *Biodiesel Separation and Purification: A Review.* Renew. Energ. 2011, 36, 437-443.

[112] Lam M.K.; Lee K.T. *Mixed Methanol–Ethanol Technology to Produce Greener Biodiesel from Waste Cooking Oil: A Breakthrough for SO_4^{2-}/SnO_2–SiO_2 catalyst*. Fuel Process. Technol. 2011, 92, 1639–1645.

[113] Lam M.; Lee K.T.; Rahman Mohamed A. *Homogeneous, Heterogeneous and Enzymatic Catalysis for Transesterification of High Free Fatty Acid Oil (Waste Cooking Oil) to Biodiesel: A Review*. Biotechnol. Adv. 2010, 28, 500–518.

[114] Georgogianni K.G.; Katsoulidis A.K.; Pomonis P.J.; Manos G.; Kontominas M.G. *Transesterification of Rapeseed Oil for the Production of Biodiesel Using Homogeneous and Heterogeneous Catalysis.* Fuel Process. Technol. 2009, 90, 1016–1022.

[115] Zhang Y.; Dube M.A.; McLean D.D.; Kates M. *Biodiesel Production from Waste Cooking Oil: 1. Process Design and Technological Assessment.* Bioresource Technol. 2003, 89, 1-16.

[116] Long Y.D.; Fang Z.; Su T.C.; Yang Q. *Co-production of Biodiesel and Hydrogen from Rapeseed and Jatropha Oils with Sodium Silicate and Ni Catalysts.* Appl. Energ. 2013, http://dx.doi.org/10.1016/j.apenergy.2012.12.076.

[117] Centi G.; Quadrelli E.A.; Perathoner S. *Catalysis for CO_2 Conversion: A Key Technology for Rapid Introduction of Renewable Energy in the Value Chain of Chemical Industries*. Energy Environ. Sci. 2013, 6, 1711-1731.

[118] Centi G.; Perathoner S. *Opportunities and Prospects in the Chemical Recycling of Carbon Dioxide to Fuels.* Catal. Today 2009, 148, 191-205.

[119] Hoffmann F.M.; Yang Y.; Paul J.; White M.G; Hrbek J. *Hydrogenation of Carbon Dioxide by Water: Alkali-Promoted Synthesis of Formate.* J. Phys. Chem. Lett. 2010, 1, 2130–2134.

[120] H. Yin, X. Mao, D. Tang, W. Xiao, L. Xing, H. Zhu, D. Wang, D.R. Sadoway. *Capture and Electrochemical Conversion of CO_2 to Value-Added Carbon and Oxygen by Molten Salt Electrolysis.* Energy Environ. Sci., 2013, 6, 1538-1545.

[121] Hu B.; Guild C.; Suib S.L. *Thermal, Electrochemical, and Photochemical Conversion of CO_2 to Fuels and Value-Added Products*. Journal of CO_2 Utilization. 2013, 1, 18–27.

[122] Kumar B.; Smieja J.M.; Kubiak C.P. *Photo-reduction of CO_2 on p-type Silicon Using Re(Bipy-But)$(CO)_3$Cl: Photovoltages Exceeding 600 mv for the Selective Reduction of CO_2 to CO.* J. Phys. Chem. C 2010, 114, 14220–14223.

[123] Bara J. *Review: The Chemistry of Amine Manufacture. What Chemicals Will We Need to Capture CO_2?* Greenhouse Gas Sci. Technol. 2012, 2, 162–171.

[124] Helwani Z.; Othman M.R.; Aziz N.; Fernando W.J.N.; Kim J. *Technology for Production of Biodiesel Focusing on Green Catalytic Techniques: A Review.* Fuel Process. Technol. 2009, 90, 1502–1515.

[125] Endalew K.; Kiros Y., Zanzi R. *Inorganic Heterogeneous Catalysts for Biodiesel Production from Vegetable Oils.* Biomass Bioenerg. 2011, 35, 3787-3809.

[126] Luque R.; Lovett J.C.; Datta B.; Clancy J.; Campeloa J.M.; Romero A.A. *Biodiesel as Feasible Petrol Fuel Replacement: A Multidisciplinary Overview.* Energy Environ. Sci. 2010, 3, 1706–1721.

[127] Ramachandran K.; Suganya T.; Gandhi N.N.; Renganathan S. *Recent Developments for Biodiesel Production by Ultrasonic Assist Transesterification Using Different Heterogeneous Catalyst: A Review.* Renew. Sust. Energ. Rev. 2013, 22, 410–418.

[128] Vyas A.P.; Verma J.L.; Subrahmanyam N. *A Review on FAME Production Processes.* Fuel 2010, 8, 1–9.

[129] Di Serio M., Ledda M., Cozzolino M., Minutillo G., Tesser R., Santacesaria E. *Transesterification of Soybean Oil to Biodiesel by Using Heterogeneous Basic Catalysts.* Ind. Eng. Chem. Res. 2006, 45, 3009-3014.

[130] Veljkovic V. B.; Stamenkovic O. S.; Todorovic Z. B.; Lazic M. L.; Skala D. U. *Kinetics of Sunflower Oil Methanolysis Catalyzed by Calcium Oxide*. Fuel 2009, 88, 554–1562.

[131] Singh Chouhan A.P.; Sarma A.K. *Modern Heterogeneous Catalysts for Biodiesel Production: A Comprehensive Review.* Renew. Sust. Energ. Rev. 2011, 15, 4378– 4399.

[132] Lee J.S.; Saka S. *Biodiesel Production by Heterogeneous Catalysts and Super-Critical Technologies: Review.* Bioresource Technol. 2010, 101, 7191–7200.

[133] Salamatinia B.; Abdullah A.Z.; Bhatia S. *Quality Evaluation of Biodiesel Produced through Ultrasound-Assisted Heterogeneous Catalytic System.* Fuel Process. Technol. 2012, 97, 1-8.

[134] Berrios M.; Martín M.A.; Chica A.F.; Martín A. *Purification of Biodiesel from Used Cooking Oils.* Appl. Energ. 2011, 88, 3625–3631.

[135] Zabeti M.; Daud W.M.A.W.; Aroua M.K. *Activity of Solid Catalysts for Biodiesel Production: A Review.* Fuel Process. Technol. 2009, 90, 770–777.

[136] Sharma Y. C.; Singh B.; Korstad J. *Latest Developments on Application of Heterogenous Basic Catalysts for an Efficient and Eco Friendly Synthesis of Biodiesel: A Review*. Fuel 2011, 90, 1309–1324.

[137] Wen Z.; Yu X.; Tu S.T.; Yan J.; Dahlquist E. *Synthesis of Biodiesel from Vegetable Oil with Methanol Catalyzed by Li-Doped Magnesium Oxide Catalysts.* Appl. Energ. 2010, 87, 743–748.

[138] Dossin T.F.; Reyniers M.F.; Berger R.J.; Marin G.B. *Simulation of Heterogeneously MgO-Catalyzed Transesterification for Fine-Chemical and Biodiesel Industrial Production*. Appl. Catal. B-Environ. 2006, 67, 136–148.

[139] Liu X.; He H.; Wang Y.; Zhu S.; Piao X. *Transesterification of Soybean Oil to Biodiesel Using CaO as a Solid Base Catalyst.* Fuel 2008, 87, 216–21.

[140] Liu X.; He H.; Wang Y.; Zhu S. *Transesterification of Soybean Oil to Biodiesel Using SrO as a Solid Base Catalyst.* Catal. Commun. 2007, 8, 1107–1111.

[141] Soares Días A.P.; Bernardo J.; Felizardo P.; Neiva Correia M.J. *Biodiesel Production by Soybean Oil Methanolysis over SrO/MgO Catalysts. The Relevance of the Catalyst Granulometry.* Fuel Process. Technol. 2012, 102, 146–155.

[142] Granados M.L.; Poves M.D.; Alonso D.; Mariscal R.; Galisteo F.C.; Moreno-Tost R. *Biodiesel from Sunflower Oil by Using Activated Calcium Oxide.* Appl. Catal. B-Environ. 2007, 73, 317–26.

[143] Watkins R.S.; Lee A.F.; Wilson K. *Li–CaO Catalysed Tri-Glyceride Transesterification for Biodiesel Applications.* Green Chem. 2004, 6, 335–340.

[144] Wang J.X.; Chen K.T.; Huang J.S.; Chen C.C. *Application of Li_2SiO_3 as a Heterogeneous Catalyst in the Production of Biodiesel from Soybean Oil.* Chinese Chem. Lett. 2011, 22, 1363–1366.

[145] Wang J.X.; Chen K.T.; Wu J.S.; Wang P.H.; Huang S.T.; Chen C.C. *Production of Biodiesel through Transesterification of Soybean Oil Using Lithium Orthosilicate Solid Catalyst.* Fuel Process. Technol. 2012, 104, 167–173.

[146] Chen K.T.; Wang J.X.; Dai Y.M.; Wang P.H.; Liou C.Y.; Nien C.W.; Wu J.S.; Chen C.C. *Rice Husk Ash as a Catalyst Precursor for Biodiesel Production.* J. Taiwan Inst. Chem. Eng. 2013, 44, 622-629.

[147] Guo P.; Zheng C.; Zheng M.; Huang F.; Li W.; Huang Q. *Solid Base Catalysts for Production of Fatty Acid Methyl Esters*. Renew. Energ. 2013, 53, 377-383.

[148] Singh A.K.; Fernando S.D. *Transesterification of Soyabean Oil Using Heterogenous Catalysts*. Energ. Fuels 2008, 22, 2067-2069.

[149] Omar W.N.N.W.; Amin N.A.S. *Biodiesel Production from Waste Cooking Oil over Alkaline Modified Zirconia Catalyst.* Fuel Process. Technol. 2011, 92, 2397-2405.

[150] Molaei Dehkordi A.; Ghasemi M. *Transesterification of Waste Cooking Oil to Biodiesel Using Ca and Zr Mixed Oxides as Heterogeneous Base Catalysts.* Fuel Process. Technol. 2012, 97, 45–51.

[151] Shibasaki-Kitakawa N., Honda H., Kuribayashi H., Toda T., Fukumura T., Yonemoto T. *Biodiesel Production Using Anionic Ion-Exchange Resin as Heterogeneous Catalyst.* Bioresource Technol. 2007, 98, 416–421.

[152] Shumaker J. L.; Crofcheck C.; Tackett S.A.; Santillan-Jimenez E.; Morgan T.; Ji Y.; Mark Crocker; Toops T.J. *Biodiesel Synthesis Using Calcined Layered Double Hydroxide Catalysts.* Appl. Catal. B-Environ. 2008, 82, 120–130.

[153] Corma A., Hamid S.B.A., Iborra S., Velty A. *Lewis and Bronsted Basic Active Sites on Solid Catalysts and their Role in the Synthesis of Monoglycerides.* J. Catal. 2005, 234, 340-347.

[154] Sankaranarayanan S.; Churchil Antonyraj A.; Kannan S. *Transesterification of Edible, Non-Edible and used Cooking Oils for Biodiesel Production Using Calcined Layered Double Hydroxides as Reusable Base Catalysts.* Bioresource Technol. 2012, 109, 57–62.

[155] Navajas A.; Campo I.; Arzamendi G.; Hernandez W.Y.; Bobadilla L.F.; Centeno M.A.; Odriozola J.A.; Gandia L.M. *Synthesis of Biodiesel from the Methanolysis of Sunflower Oil Using PURAL® Mg–Al Hydrotalcites as Catalyst Precursors.* Appl. Catal. B-Environ 2010, 100, 299–309.

[156] Gomes J.F.P.; Puna J.F.B.; Gonçalves L.M.; Bordado J.C.M. *Study on the use of MgAl Hydrotalcites as Solid Heterogeneous Catalysts for Biodiesel Production.* Energy 2011, 36, 6770-6778.

[157] Sánchez-Cantú M.; Pérez-Díaz L.M.; Tepale-Ochoa N.; González-Coronel V.J.; Ramos-Cassellis M.E.; Machorro-Aguirre D.; Valente J.S. *Green Synthesis of Hydrocalumite-Type Compounds and their Evaluation in the Transesterification of Castor Bean Oil and Methanol*. Fuel 2013, 111, 23-31.

[158] Sun H.; Ding Y.; Duan J.; Zhang Q.; Wang Z.; Lou H.; Zheng X. *Transesterification of Sunflower Oil to Biodiesel on ZrO_2 Supported La_2O_3 Catalyst.* Bioresource Technol. 2010, 101, 953–958.

[159] Kim H.J.; Kang B.S.; Kim M.J.; Park Y.M.; Kim D.K.; Lee J.S.; Lee K.Y. *Transesterification of Vegetable Oil to Biodiesel Using Heterogeneous Base Catalyst.* Catal. Today 2004, 93–95, 315–320.

[160] Ebiura T.; Echizen T.; Ishikawa A.; Murai K.; Baba T. *Selective Transesterification of Triolein with Methanol to Methyl Oleate and Glycerol Using Alumina Loaded with Alkali Metal Salt as a Solid-Base Catalyst*. Appl. Catal. A-Gen. 2005, 283, 111–116.

[161] Xie W.; Li H. *Alumina-Supported Potassium Iodide as a Heterogeneous Catalyst for Biodiesel Production from Soybean Oil.* J. Mol. Catal. A-Chem. 2006, 255, 1–9.

[162] Lukic I.; Krstic J.; Jovanovic D.; Skala D. *Alumina/Silica Supported K_2CO_3 as a Catalyst for Biodiesel Synthesis from Sunflower Oil.* Bioresource Technol. 2009, 100, 4690–4696.

[163] Evangelista J.P.C.; Chellappa T.; Coriolano A.C.F.; Fernandes Jr. V.J.; Souza L.D.; Araujo A.S.; *Synthesis of Alumina Impregnated with Potassium Iodide Catalyst for Biodiesel Production from Rice Bran Oil.* Fuel Process. Technol. 2012, 104, 90–95.

[164] Arzamendi G.; Campo I.; Arguiñarena E.; Sánchez M.; Montes M.; Gandía L.M. *Synthesis of Biodiesel with Heterogeneous NaOH/Alumina Catalysts: Comparison with Homogeneous NaOH.* Chem. Eng. J. 2007, 134, 123–130.

[165] Baroutian S.; Aroua M.K.; Raman A.A.; Sulaiman N.M.N. *Methanol Recovery During Transesterification of Palm Oil in a TiO_2/Al_2O_3 Membrane Reactor: Experimental Study and Neutral Network Modeling*. Sep. Purif. Technol. 2010, 76, 58–63.

[166] Wu H.; Zhang J.; Wei Q.; Zheng J.; Zhang J. *Transesterification of Soybean Oil to Biodiesel Using Zeolite Supported CaO as Strong Base Catalysts.* Fuel Process. Technol. 2013, 109, 13-18.

[167] Babajide O.; Musyoka N.; Petrik L.; Ameer F. *Novel Zeolite Na-X Synthesized from Fly Ash as a Heterogeneous Catalyst in Biodiesel Production.* Catal. Today 2012, 190, 54-60.

[168] Alves C.T.; Oliveira A.; Carneiro S.A.V; Silva A.G.; Andrade H.M.C.; Vieira de Melo S.A.B.; Torres E.A. *Transesterification of Waste Frying Oil Using a Zinc Aluminate Catalyst*. Fuel Process. Technol. 2013, 106, 102–107.

[169] Borges M.E.; Díaz L. *Recent Developments on Heterogeneous Catalysts for Biodiesel Production by Oil Esterification and Transesterification Reactions: A Review.* Renew. Sust. Energ. Rev. 2012, 6, 2839–2849.

[170] Di Serio M.; Tesser R.; Pengmei L.; Santacesaria E. *Heterogeneous Catalysts for Biodiesel Production.* Energ. Fuels 2008, 22, 207–17.

[171] Wen Z., Yu X., Tu S.T., Yan J., Dahlquist E. *Biodiesel Production from Waste Cooking Oil Catalyzed by TiO_2–MgO Mixed Oxides.* Bioresource Technol. 2010, 101, 9570–9576.

[172] Guo F.; Peng Z.G.; Dai J.Y.; Xiu Z.L. *Calcined Sodium Silicate as Solid Base Catalyst for Biodiesel Production*. Fuel Process. Technol. 2010, 991, 322–328.

[173] Singh A.K.; Fernando S.D.; Hernandez R. *Base Catalyzed Fast Transesterification of Soybean Oil Using Ultrasonication.* Energ. Fuel 2007, 21, 1161–1164.

[174] Kalva A.; Sivasankar T.; Moholkar V.S. *Physical Mechanism of Ultrasound-assisted Synthesis of Biodiesel*. Ind. Eng. Chem. Res. 2008, 48, 534–544.

[175] Nishimura CSMV; Maeda Y.R. *Conversion of Vegetable Oil to Biodiesel Using Ultrasonic Irradiation.* Chem. Lett. 2003, 32, 716–717.

[176] Salamatinia B., Mootabadi H., Bhatia S., Abdullah A.Z. *Optimization of Ultrasonic-Assisted Heterogeneous Biodiesel Production from Palm Oil: A Response Surface Methodology Approach.* Fuel Process. Technol. 2010, 91, 441–448.

[177] Mootabadi H.; Salamatinia B.; Bhatia S.; Abdullah A.Z. *Ultrasonic-assisted Biodiesel Production Process from Palm Oil Using Alkaline Earth Metal Oxides as the Heterogeneous Catalysts*. Fuel 2010, 89, 1818–1825.

[178] Deng X.; Fang Z.; Liu Y.; Yu C. *Production of Biodiesel from Jatropha Oil Catalyzed by Nanosized Solid Basic Catalyst.* Energy 2011, 36, 777–784.

[179] Deng X.; Fang Z.; Hu Y.; Zeng H.; Liao K.; Yu C.L. *Preparation of Biodiesel on Nano Ca–Mg–Al Solid Base Catalyst under Ultrasonic Radiation in Microaqueous Media*. Petrochemical Technology 2009, 38, 1071–1075.

IntechOpen